[Frontiers in Bioscience, Landmark, 18, 36-57, January 1, 2013]

Steps of the coupled charge translocation in the catalytic cycle of cytochrome *c* oxidase

Sergey A. Siletsky[1]

[1]*A.N.Belozersky Institute of Physico-Chemical Biology, Moscow State University, Moscow 119992, Russia*

TABLE OF CONTENTS

1. ABSTRACT

Cytochrome *c* oxidase (COX) terminates the respiratory chain in mitochondria and in plasmatic membrane of many aerobic bacteria. The enzyme reduces dioxygen molecule into water and the reaction is accompanied with generation of transmembrane difference of electric potentials. The energy conservation by COX is based on the vectorial organization of the chemical reaction due to substrate protons transfer from the negative phase into the active site to meet the electrons, coming from opposite side of the membrane. In addition, a half of free energy of redox-chemistry reaction is conserved through transmembrane proton pumping. Each of the reaction steps in the catalytic cycle of COX involves a sequence of coupled electron and proton transfer reaction. The time-resolved study of the coupled charge translocation during catalytic cycle of cytochrome *c* oxidase is reviewed. Based on many fascinating parallels between the mechanisms of COX and pigment-protein complex of photosystem II from oxygenic photosynthetic organisms, the data described could be used in the light-driven water-splitting process.

2. INTRODUCTION

2.1. The overall characterization of cytochrome oxidase

Terminal oxidases constitute the last component of the respiratory chains in eukaryotes and aerobic prokaryotes (1-2). These wide-spread membrane-bound enzymes catalyze oxygen reduction by cytochrome *c* or ubiquinone, coupled to formation of transmembrane electrochemical proton gradient (protonmotive force or $\Delta\mu H^+$), which is required for synthesis of ATP (3-4).

The main subgroup of terminal respiratory oxidases is a superfamily of structurally related heme-copper oxidases, in which the catalytic oxygen-reduction site is formed by the heme group and copper ion in close proximity (the so called binuclear centre, BNC). Members of the superfamily of heme-copper oxidases can be divided into 3 large groups denoted as A-, B- and C-type families differing mainly in the structure of proton channels (5).

The most thoroughly explored canonical cytochrome *c* oxidases (COXs), including enzyme from

bovine heart mitochondria, aa_3 oxidases from *Paracoccus denitrificans* and *Rhodobacter sphaeroides* belong to the A-family (4, 6-11). The mitochondrial-like cytochrome *c* oxidases contain four redox-centres. The binuclear catalytic site is buried within the hydrophobic core of the protein and comprised of two redox centres: a high-spin iron of the heme a_3 and copper ion (Cu_B). Two other input centers of COX, Cu_A and low-spin heme *a* transfer electrons step by step from the natural electron donor, cytochrome *c* at positive side of the membrane to the BNC, where each molecule of dioxygen is reduced to the two waters.

By tradition, the oxygen-binding heme is designated with a subscript "3". In bacteria, heme groups can be presented by different heme types: *a* or *b* for the low-spin and a_3, o_3, or b_3 for the high-spin heme, correspondingly. To a lesser extent studied ba_3 cytochrome *c* oxidase from *Thermus thermophilus* exemplifies the B-type family enzymes (12-14). Some bacterial oxidases may have extra hemes of *c*-type. The most distant C-family is constituted by the cbb_3 oxidases from various species (15-17). Recently, a detailed comparative genomic analysis and structural modeling has identified 5 more additional families (D, E, F, G, and H), found exclusively in Archaea (18).

During turnover of COX, the $\Delta\mu H^+$ is generated by two different ways. Firstly, in the course of dioxygen reduction to water, the so-called "substrate" (or "chemical") protons are taken up electrogenically from the inner (negative, N-side) aqueous phase to the BNC, where they combine with the electrons, coming from cytochrome *c* on the opposite side (positive, P-side) of the membrane (19). Secondly, in addition to uptake of the substrate protons, a single proton is pumped electrogenically across the membrane for each electron transferred by cytochrome oxidase to dioxygen ("pumped" protons), as it was discovered by Wikström (20-21).

$$4c^{2+} + O_2 + 8H^+_{in} \rightarrow 4c^{3+} + 2H_2O + 4H^+_{out}$$

Thus, the reaction is coupled to a charge separation corresponding to net unidirectional transfer of 8 charges across the membrane for the each molecule of oxygen reduced. The molecular mechanism of the redox-linked electrogenic transfer of the chemical and pumped protons has been a basic problem in studies of the cytochrome oxidase mechanism for more than 30 years (11).

2.2. Crystallographic structure

Three-dimensional crystal structure of several representatives of the A-type family has been determinated by X-ray crystallography. These are COX from bovine mitochondria (22-25), bacterial aa_3-type cytochrome oxidases from *Paracoccus denitrificans* (26-28) and *Rhodobacter sphaeroides* (29-30), the quinol oxidase from *Esherichia coli* (31). Besides, the atomic structure was resolved for cytochrome ba_3 from *Thermus thermophilus* (13, 32) and cytochrome cbb_3 from *Pseudomonas shutzeri* (17).

All representatives of the heme-copper terminal oxidases share a central largest subunit I built up of 12 membrane-spanning helices. The COX from bovine mitochondria contains 13 subunits, while the bacterial enzymes are usually made up of no more than four peptides. Mitochondrial DNA encodes three largest subunits that form a core of enzyme. The subunit I contains three redox-active cofactors: a low-spin heme group *a*, high-spin heme a_3 and Cu_B. The center-to-center distance between heme *a* and heme a_3 is around 13 Å, whereas they are within Wan der Waals contact at the edges that provides a basis for rapid electron transfer (33). A distance between constituents of the catalytic BNC, the Fe atom of the high-spin heme and copper atom of Cu_B is about ~ 4.5-5 Å (13, 17, 22, 26).

Low-spin heme and binuclear centre are located at about the same depth in the membrane, of about one third of the membrane thickness from the P-side (22, 26). The hemes are oriented perpendicular to the membrane plane, such that its propionate moieties are pointing to the P-side. Two other substituents of the heme *a* and a_3 (formyl group and hydroxyethylfarnesyl side chain) are pointing to the N-side of the membrane. The copper atom of Cu_B is retained in the protein by ligation with three histidines (H284, H333 and H334; amino acid numbering from *R.sphaeroides* is used). There is a crosslink between one of the Cu_B histidine ligands (His284) and a tyrosine residue (Y288) (23, 34-35), which is suggested to supply a proton to promote scission of the O-O bond and may be included as part of the catalytic site (36-38).

The low-spin heme *a* is an immediate electron donor for the heme a_3/Cu_B site. It is re-reduced by Cu_A, redox-active center composed of two copper ions. The Cu_A is held by subunit II of COX, which has two membrane spanning α-helices and provides a docking surface for cytochrome *c* at the positive side of the membrane. Comprised from seven transmembrane helices, the third subunit does not hold any redox-active metal sites, but it is highly conserved. In absence of this subunit the catalytic cycle of cytochrome oxidase is 100-1000 fold less and the enzyme undergoes suicide inactivation (39).

From the N-side of the membrane, substrate and pumped protons are delivered through the special conducting pathways to the binuclear catalytic site and to the P-side of the membrane, correspondingly. Crystal structures of COXs from different sources (13, 22, 26, 29) reveal three "pores" (the so called "K-", "D-", and "H-channels") situated in the subunit I. The D-pathway is named after a highly conserved aspartate residue (D132) at the entrance of the "channel" (Figure 1) (40-42). The pathway leads through the clear chain of ~10-12 hydrogen-bonded water molecules (28-30) to the another highly conserved acidic residue (E286) located about 10-12 Å from the heme-copper centre and about 24-26 Å from the D132 (29). The water molecules are stabilized by hydrogen bonds to a series of hydrophilic conserved residues: N139, N121, N207, S142, S200, S201, and S197 (43).

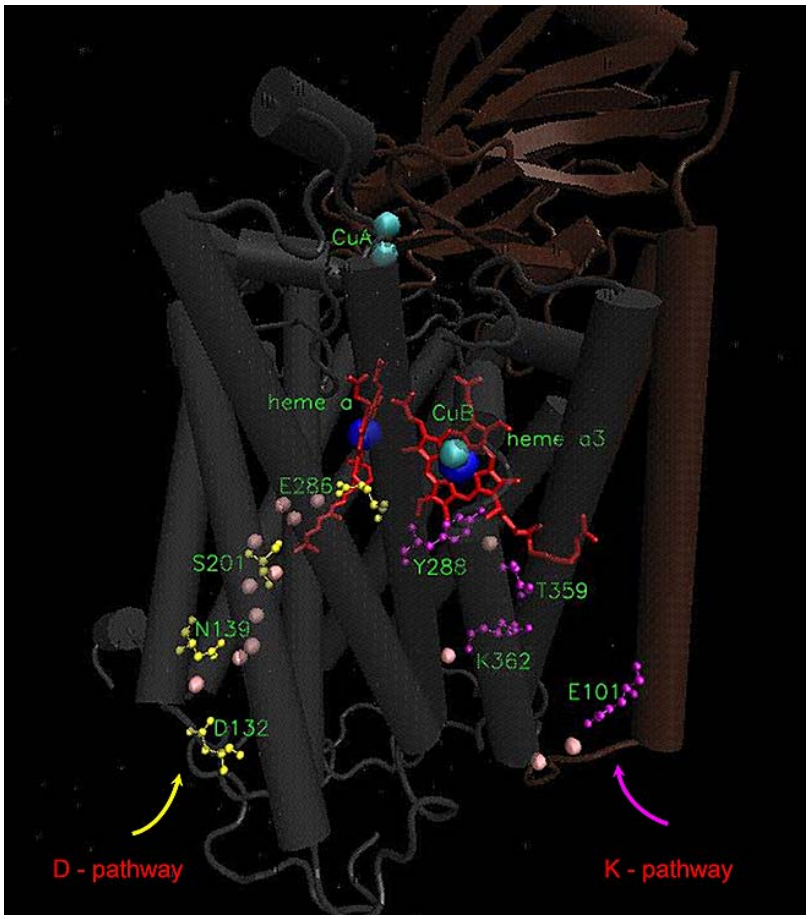

Figure 1. The overall structure of cytochrome *c* oxidase. The two subunits (I and II) of the *R. sphaeroides* wild type cytochrome *c* oxidase are shown in different colors. The redox-active cofactors and several conserved residues in the D and K proton pathways are indicated. Water molecules resolved in the D path are displayed as small pink spheres. The structure was obtained from Protein Data Bank (29). The picture was prepared with the aid of Visual Molecular Dynamics software from Amersham Biosciences (173).

The K-pathway is named after a highly conserved lysine residue (K362) in the middle of the pahway (Figure 1) (41-42). Resolved in the X-ray crystal structure, this pathway leads from surface of the protein at the N-side to the Y288 residue in close proximity to the binuclear center. The entry point to the K pathway is formed by the E101 residue of subunit II (44) or by the chain from four water molecules, stabilized by E101 without direct involvement of this residue in proton transfer (28). In addition to the lysine, this pathway includes a highly conserved threonine residues (T352 and T359) and a tightly bound few (two or three) water molecules. The chain of hydrogen bonds is interrupted by a gap between K362 and T359 residues, which could be bridged by the side chain movement of the lysine residue (28, 45).

A third, H-channel has been defined for the mammalian cytochrome oxidase and has been proposed to be used for pumping of protons, providing a possible pathway from the N-side to the residue D51 located on the P-side of the membrane (24-25, 46). Though the major structural features of H-pathway can be found in bacterial enzymes of A family (cytochromes aa_3 from *P. denitrificans* and *R. sphaeroides* and cytochrome bo_3 from *E. coli*) (9, 11), the crucial for the proposed mechanism, D51 residue is not conserved. To this time, extensive site-directed mutations of residues in the H-pathway of bacterial oxidases are believed to exclude its importance in function of the prokaryotic enzymes (4, 6, 11, 47-48).

There is no visible proton connectivity in the crystallographic structure of the D-channel beyond E286 (22, 26). A proton transfer through a short series of waters is modeled in the nonpolar cavity between E286 and the active site (49-51), while the only one bound water molecule was defined by the X-ray crystallography (30). Arrays of 3-4 mobile water molecules are suggested to form the proton-conductive pathway and to assist proton transfer from E286 either to the so-called proton-loading site (PLS, situated near propionates of heme a_3) for pumping or to the BNC for water formation (49, 52).

Proton-loading site (PLS) is proposed to be a temporally store site for the pumped proton. The precise

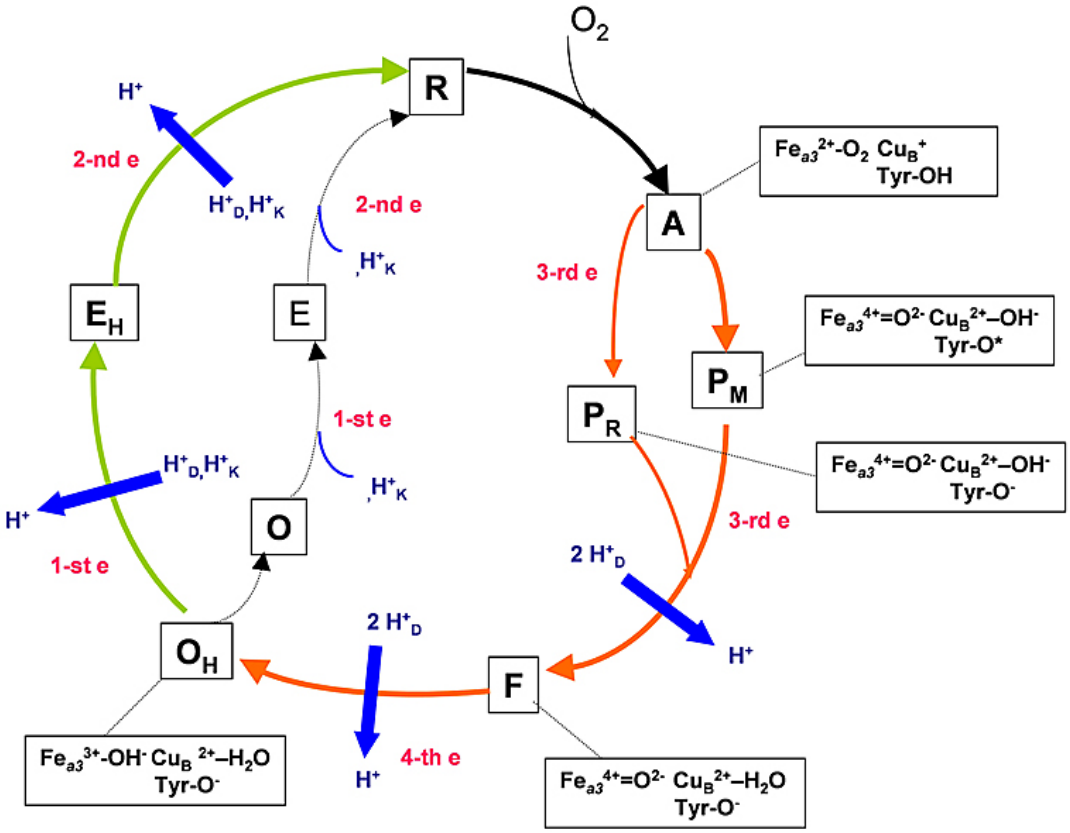

Figure 2. Scheme of the catalytic cycle of A-family cytochrome *c* oxidase. Transitions from R to O_H form the oxidative part, while transitions from O_H to R form the reductive part of the cycle. For the oxidative halve of the reaction, the likely structure of intermediates of the binuclear centre, including redox-active tyrosine residue, are shown. Protons, supplied during catalytic cycle by the D- and K pathways are indicated as H_D^+ and H_K^+, correspondingly.

place of the PLS is not determined yet. The prime candidates are the A-propionate of heme a_3 and one of the histidine ligands to Cu_B (H334 in *R.sphaeroides*) (53-56). Release of the pumped proton out of the enzyme occurs by putative multiple exit pathways through the highly hydrophilic domain above the heme groups and Cu_B (57) that involves several arginines, propionates of hemes, bound non-redox active metal centres and water molecules (28) .

The oxygen transfer pathway is organized by the several hydrophobic passages from the middle of the membrane bilayer toward the active site (22, 29, 58-59). There is indications that pathway for water exiting from the binuclear centre lead to the vicinity of Mg^{2+}/Mn^{2+} site (non-redox active metal ion) above the heme groups, at the interface between subunits I and II (60), and may be involved in the proton exit pathway (61).

2.3. Catalytic cycle

Starting with the fully oxidized cytochrome oxidase, the catalytic redox cycle of the enzyme binuclear center can be depicted schematically as follows, where O, E, R, Oxy, P_M and F are intermediate states of the active site.

$$\underset{\mathbf{O}\ \text{(Oxidized)}}{} \xrightarrow{\text{First 2 e}^-} \underset{\mathbf{E}}{} \rightarrow \underset{\mathbf{R^2}\ \text{(Reduced)}}{} \xrightarrow{O_2} \underset{\mathbf{Oxy}\ \text{(Oxygenated)}}{} \rightarrow$$

$$\underset{\mathbf{P_M}\ \text{(“Peroxy”)}}{} \xrightarrow{\text{3-rd e}^-} \underset{\mathbf{F}\ \text{(Ferryl-Oxo)}}{} \xrightarrow{\text{4-th e}^-} \underset{\mathbf{O}\ \text{(Oxidized)}}{}$$

Formally, the catalytic cycle of cytochrome oxidase can be divided into the two halves: oxidative (R→…) and reductive (…→R) (Figure 2). During the reductive phase (O→E and E→R transitions), the input of two electrons reduces the binuclear center that enables binding of dioxygen to the central iron of high spin heme a_3. Binding of O_2 to heme a_3 initiates formation of the oxycomplex, referred to as compound A (62), which is a mixture of Fe^{2+}-O_2 and Fe^{3+}-O_2^- species (63). This is followed by splitting of the O-O bond and generation of the P_M intermediate (usually termed “peroxy”), which requires transfer of the four electrons and at least one proton from the active site moieties to the O_2. Two electrons are provided by heme a_3 Fe^{2+}, which is oxidized to a hypervalent oxoferryl heme a_3 $Fe^{4+}=O^{2-}$ (64-65). One electron is provided by Cu_B^+, which is oxidized to Cu_B^{2+}. The forth electron and a proton are believed to be provided by the tyrosine 288, which is covalently bonded to one of the histidine ligands (His-284) of Cu_B (23, 34-35).

Donation of the proton and electron results in a neutral tyrosyl radical (Figure 2) (36-37). The tyrosine may not be sole redox-active amino acid residue (66-68). A radical form of the highly conserved tryptophan (W280), which forms a π-stacking interaction with His-334 ligand of Cu_B was detected that suggest the possibility of fast migration of the radical generated in the catalytic active site of COX (66, 69). After O_2 reacts with the reduced form of binuclear center to produce the P_M intermediate, single electron reduction by the 3rd and 4th electrons delivered one by one from cytochrome *c* generates correspondingly state F (referred usually as "ferryl-oxo") and then the fully oxidized state O (or O_H) (Figure 2). O_H is the so-called "high-energy" oxidized state found recently during study of oxidation of the fully reduced COX.

If oxygen binds to heme a_3 of the fully (four electron) reduced cytochrome oxidase, the P_M state is not resolved. In this case, generation of compound A (62) is followed by the fast electron transfer from the heme *a* to BNC, which is believed to reduce rapidly the tyrosine radical into tyrosinate anion (70), forming P_R state (Figure 2) (71-72). The P_R state has presumably the same chemical structure as P_M but with one additional electron in BNC (36-37, 42, 73) and it decays spontaneously into F, accompanied by the proton uptake from solution. After formation of the F state the last electron transfer from the equilibrated heme *a*/Cu_A pair reduces the F state of BNC to complete formation of the oxidized state (O_H).

In absence of electron donors the just oxidized state (O_H) relaxes into the oxidized ground state (O) that is different from the O_H state by the electron affinity of redox-centres (74-78). Immediate reduction of the O_H state results in electron delivery to the optically invisible Cu_B center with formation of the one-electron reduced E_H state (75-78), whereas single-electron injection into the ground O state of COX is limited by the heme *a* reduction (79-80). The optical spectra of the O and O_H states are very similar (81), which leaves the question of structural difference between these two states open.

2.4. Approaches to study the charge transfer events in cytochrome oxidase with time-resolution

The single turnover of COX occurs in the milliseconds time domain. Two main approaches were introduced to start synchronously the electron transfer process in the whole ensemble of protein molecules by the short-time laser flash. The so called "flow-flash" method is a combination of the conventional stopped-flow technique with laser-induced initiation of the reaction (82). During the measurements, reduced and CO-inhibited cytochrome oxidase is mixed in a stopped-flow apparatus with an oxygen-containing buffer in the dark. A strong laser pulse thereafter is used to dissociate CO from heme a_3 allowing dioxygen to bind and to begin the reaction simultaneously in all cytochrome oxidase molecules present. In fact, this method allows studying the oxidation of COX by molecular oxygen in the single-turnover regime, though the only oxidative part of the catalytic cycle can be normally monitored with time resolution (71-72, 83).

The second approach is based on injection of a single electron into the enzyme with help of photo-activated ruthenium derivatives, initially developed by Gray and coworkers (84-89) or by using of pulsed-radiolysis technique (90-91). In fact, this method allows studying separately the single-electron steps in the catalytic cycle of enzyme, trapped at different intermediate states of the catalytic cycle before electron injection. Nilsson adopted this methodology for use with cytochrome *c* oxidase (87), studying the rates of electron transfer in different states of the enzyme.

After triggering of the reaction, the following transitions can be monitored by the UV-vis spectroscopy (71-72, 82-83, 87), resonance Raman (64), capacitive potentiometry (92-95), and so on. For studying of the electrogenic steps, the time-resolved electrometric method (or capacitive potentiometry) was developed by L.A. Drachev and coworkes in Belozersky Institute of the Physico-Chemical Biology and was applied originally for bacterial reaction centers and bacteriorhodopsin (92-93). The principle of this method is based on the recording with time-resolution of the voltage across a lipid-coated thin collodian film with adhered to the one side of the film, the reconstituted proteoliposomes. The amplitude of the $\Delta\Psi$ across the measuring membrane is increased proportionally to that of the proteoliposomal membrane allowing the kinetics of charge translocation to be followed.

At the first time, the charge transfer steps during F→O transition of bovine heart cytochrome oxidase have been monitored with time-resolution by D. Zaslavsky, A.D. Kaulen and coworkers (94, 96). The electrometric method was applied (92-93), and a single-electron injection into cytochrome oxidase carried out with help of the lazer induced tris(2,2-bipyridyl) ruthenium complex (Rubpy), as was described initially by Nilsson (87). Later, this technical approach was expanded to the COX trapped at the P_M state (3-rd electron in the catalytic cycle) and fully oxidized state (79-80, 97). Apart from the mammalian COX, this approach was exploited for the mutant forms of bacterial COX from *R.sphaeroides* (41, 98-100) and from *P.denitrificans* (80, 101-102).

In the Helsinki Bioenergetics group, at the first time the time-resolved electrometric technique was combined with the "flow-flash" method by M. Verkhovsky and coworkes (95), and electrogenic steps coupled to oxidation of the fully reduced COX by oxygen in the single-turnover regime were studied extensively (4, 95, 103-105). The most recently, the Helsinki group combined the "flow-flash" method and photoreduction by using of Rubpy in order to investigate the single-electron injection into the metastable O_H (just oxidized) state of cytochrome oxidase (74-75).

3. CHARGE TRANSFER EVENTS COUPLED TO THE PARTIAL SINGLE-ELECTRON STEPS IN THE CATALYTIC CYCLE OF THE A FAMILY CYTOCHROME OXIDASES

In this topic, it is reviewed the time-resolved studies of intraprotein charge translocation coupled to different single electron steps of the catalytic cycle. The main attention is focused on the electrometric data.

3.1. R→A transition

If the enzyme is reduced by two electrons, the oxygen can bind to the binuclear centre and react. The initial spectroscopically detectable intermediate, A state of enzyme (62, 106) forms within 10 μs (with 1 mM O_2) (72). The resonance Raman Fe-O_2 stretch spectrum of the A intermediate is similar to that found in oxyhemoglobin and oxymyoglobin (107-108). This step does not generate a transmembrane voltage and is not associated with proton uptake or release. During reaction of the fully reduced enzyme with oxygen in the single-turnover regime, the kinetics of membrane potential generation of the incorporated into proteoliposomes *aa₃* oxidase starts from the lag-phase (103-104), which involves the electrically silent release of CO and binding of dioxygen with formation of compound A (62, 109).

3.2. A→P_R transition

If the additional (third) electron is present on heme *a* of enzyme before reaction with oxygen, generation of the compound A is followed by electron transfer from heme *a* to BNC, forming P_R state (Figure 2) (71-72). Starting from the fully reduced enzyme, this transition develops with a time constant of ~25-40 μs and is accompanied by the parallel vectorial charge movement, which amounts to transfer of one electrical charge across about 30% of the membrane dielectric (110). The charge translocation is suggested to be mainly due to internal proton transfer from the E286 residue to an unidentified acceptor above the heme groups (presumably to the PLS) (111), which may be the initial step of the proton pump mechanism of COX (11, 99, 111-112). Though some charge reorganization within the protonic K pathway during A→P_R transition can not be excluded, which may probably facilitate reduction of the catalytic site (113).

Besides, the breaking of the oxygen-oxygen bond during the P_R formation requires delivery of a chemical proton from the closely located redox-active tyrosine residue (Y288) to the catalytic site (114), which may explain the charge translocation across up to the 10% of the membrane dielectric (115).

3.3. A→P_M transition

This transition can be resolved, starting the reaction with oxygen from the two-electron reduced COX. Three out of four electrons required for oxygen reduction at this stage are taken from the BNC, whereas the fourth electron and a proton are provided by the cross-linked tyrosine (70). Since both electron and proton goes in the same direction and distance, the A→P_M transition does not generate a transmembrane voltage and virtually no phase of potential generation during R→A→P_M steps has been obtained using the electrometric technique (103).

3.4. P_R→F transition

The P_R→F transition can be monitored through study of the oxidation of the three or four-electron (fully) reduced COX by molecular oxygen in the single-turnover regime. The BNC possess the same amount of electrons in the P_R and F states of enzyme. So, the P_R→F transition includes only the proton transfer from the N-phase to the vicinity of heme *a₃*, most likely to the Cu_B bound hydroxyl (114-116), which results in the change of the α-band spectrum of the ferryl compound of heme *a₃* (shift of the peak from 607 to 580 nm). The P_R→F transition is accompanied by the electron re-equilibration from Cu_A to the low-spin heme *a*. Besides, P_R→F transition is linked to proton pumping across the membrane (95, 103-104), the initial part of which is associated with A→P_R transition (111).

The corresponding phase of the membrane potential generation during the time-resolved reaction of fully-reduced bovine and bacterial *aa₃* cytochrome oxidases with molecular oxygen develops with rate constant τ ~30-100 μs. The amplitude of voltage formed during the overall A→P_R→F transition (111) is about half of the total membrane potential generated during the oxidative part of the reaction (95, 103, 117). The precise number of charges transferred across the membrane during the reaction can be defined from the calibration. For this purpose, the parallel measurement of the electron transfer from the low-spin heme to Cu_A can be used, following CO photolysis in the absence of oxygen ("backflow" process) (103). Assuming initially that transfer of an electron from the low-spin heme to Cu_A amounts to movement of a unit charge across half of the membrane dielectric (118), the value of 5.5 unit charges translocation during A→P_R→F→O transitions was obtained - the value predicted if all four protons pumped during the catalytic cycle are translocated during the oxidative part of the reaction (103).

However, this estimation was carried out to be overestimated. Later, by using of the value of one third for the dielectric distance between low-spin heme and Cu_A, dedicated from the X-ray crystallographic structure (26, 119) and experimental determination (74, 104, 110, 120), the P_R→F step was assumed to be coupled to transfer through the membrane of about 1.3-1.6 charges and of about two charges during consecutive A→P_R→F transitions (104, 111, 117). By the direct measuring of pH changes, it has been shown recently that P_R→F transition is associated with uptake of two protons from the inside solution of the COX incorporated proteoliposomes and release of the one proton to the outer bulk phase (121).

3.5. P_M→F transition

This transition corresponds to transfer of the 3rd electron in the catalytic cycle and can be observed during the single-electron injection into the cytochrome oxidase, converted initially to the P_M state by the special CO treatment (79, 122). As was shown, the reaction generates a voltage across the membrane in several kinetic phases. The first electrogenic phase of the mitochondrial enzyme with rate constant ~ 40-50 μs and relative amplitude of about 20%, reflects electrogenic transfer of electron from Cu_A to heme *a*. This component is not inhibited by cyanide, which binds to the oxidized heme a_3 and prevents the electron reduction of the BNC. Following the electrogenic reduction of heme *a*, the subsequent generation of voltage during P_M→F transition is formed by two components of proton movement with time-constants of approximately 0.3 ms and 1.3 ms coupled to electron transfer from heme *a* to

the heme a_3. The electron transfer between hemes does not contribute by itself into the membrane potential generation, since it is directed in parallel to the membrane surface.

The two resolved KCN-sensitive protonic phases are characterized by the relative amplitudes with ratio of about 1:2.4 (122). The rates of phases associated with $P_M \rightarrow F$ transition are slower as compared to the $P_R \rightarrow F$ transition (~80 μs phase in mitochondrial enzyme (103)) that can be explained by difference in the reduced state of binuclear centre in P_M and P_R intermediates (79, 123). While P_M state of BNC is two-electron deficient relative to the oxidized enzyme, the P_R is a state in which the additional electron has been accepted by the BNC. Thus the $P_R \rightarrow F$ transition is rate-limited by the pure internal proton transfer step, presumably by the deprotonation of the conserved glutamate residue (E286) at the top of D-channel (124-126).

Meanwhile, the $P_M \rightarrow F$ transition is induced and limited by the proton-coupled electron reduction of BNC from heme *a,* the rate of which is delayed proportionally to the low quasi-equilibrium occupancy of the reduced BNC in the P_M state (123, 127).

3.6. $F \rightarrow O_H$ transition

The $F \rightarrow O_H$ transition can be resolved both during single-electron injection experiments (87, 94, 128) and in the course of fully-reduced COX reaction with oxygen in the single-turnover regime (95, 103).

Mitochondrial enzyme. Before electron injection, the oxidized enzyme can be fully converted to the stable ferryl-oxo state by addition of excess hydrogen peroxide (94, 129). Photoinjection of a single-electron from RuBpy into COX from bovine heart mitochondria, poised at the ferryl-oxo F state converts the enzyme to the oxidized (O) form and gives rise to 3 major electrogenic phases (94). The "rapid" electrogenic phase (τ_1 ~ 40-50 μs, 20% of the total amplitude) shows very weak temperature dependence (E_a~ 3.6 kcal/mol**)** (130), which coincides with that of the rate constant of the heme *a* reduction by the Cu_A in the pulsed-radiolysis measurements (90, 131) and points most probably that neither bond making or breaking occurring (132). The measured rate (87, 94, 128) is in agreement with the electron transfer from Cu_A to heme *a* due to pure tunneling (133). It does not depend on pH, is not affected by the H_2O/D_2O-replacement. Thus it is most probably not coupled with synchronous proton movement (4, 99, 101, 130).

In contrast to the microsecond ("rapid") electrogenic phase, the following "intermediate" (τ_2 ~ 1.2 ms, r.a. ~ 20%) and "slow" (τ_3 ~ 4.5 ms, r.a. ~ 60%) components demonstrate the high values of the energy activation (~ 17 and ~ 19 kcal/mol, correspondingly (130)). These electrogenic steps are sensitive to KCN and originate in the vectorial proton transfer coupled to reoxidation of heme *a* by the ferryl-oxo complex of heme a_3, in agreement with significant H_2O/D_2O kinetic solvent isotope effect (99). Similar values of activation energies have been observed for light-driven and redox-driven intraprotein proton translocation (134-138). Taken alone, a proton transfer across the continuous network of hydrogen bonds has a relatively small value of activation energy, close to that of a diffusion-controlled reaction (~ 2–3 kcal/mol) (139). Hence, a high value of activation energy should be attributed to structural changes in the proteins accompanying the intraprotein proton translocation (137).

The "slow" electrogenic phase is decelerated 6-7-fold by ions of zinc added from the outside of proteoliposomes (140). Studies on the photosynthetic reaction centers (141), bc_1 complex (142), voltage-gated proton channels (136), as well as binding of Zn^{2+} ions at the matrix side of cytochrome oxidase (143-144) showed that zinc addition may inhibit uptake of protons from bulk phase due to competition of zinc ions and protons for a binding site on the external surfaces of the H^+ transfer pathways. The specific effect of Zn^{2+} ions from the P-side of the membrane indicates for the "slow" electrogenic phase to be specifically associated with release of the pumped proton to the output phase.

The electron transfer from Cu_A to heme *a*, being reflected by the rapid electrogenic component may serve as internal standard in order to define the number of charges transferred across the membrane during single-electron reaction (94). Based on the coincidence of the amplitude of the "rapid" electrogenic phase (~ 20%), the overall number of charges translocated across the membrane during the $P_M \rightarrow F$ and $F \rightarrow O$ single-electron steps is shown to be equal (79, 116). Meanwhile, both of protonic phases coupled to transfer of the 3rd electron are 3-4-fold faster than observed for transfer of the 4th electron (79, 145). The discrepancy can be reasonably explained by the different redox chemistry at the active site, namely due to the higher midpoint redox potential of the electron acceptor, the tyrosine radical ($P_M \rightarrow F$ transition) as compared to the oxoferryl heme a_3 ($F \rightarrow O$ transition) (Figure 2) (123, 146).

The very similar magnitude ratio of the two main protonic phases ("intermediate" and "slow") is observed for both of $F \rightarrow O$ and $P_M \rightarrow F$ transitions. It is approximated ~1:3 and 1:2.4 correspondingly (79, 94). It is significant that the rate constants of the"intermediate" and "slow "electrogenic components differ by less than an order of magnitude. Hence, if the two protonic phases occur in series, rather than in parallel (which is likely to be the case), the true magnitude values, A_2 and A_3, need to be calculated from the observed values, $A_{2\ (obs)}$ and $A_{3\ (obs)}$, according to the equations 1 and 2 (122, 147):

$$A_2 = A_{2(obs)} + A_{3(obs)} \times k_3/k_2 \quad \text{(eq. 1)}$$

$$A_3 = A_{3(obs)} \times (k_2-k_3)/k_2 \quad \text{(eq. 2)}$$

The recalculated values of the two electrogenic protonic phases have similar magnitudes (A_2/A_3 = 1:1.2-1:1.3) for both of the single-electron steps $P_M \rightarrow F$ and $F \rightarrow O$ in mitochondrial oxidase.

In the "flow-flash" induced reaction of the fully reduced aa_3 oxidases with O_2 (single-turnover regime), the $F \rightarrow O$ transition is a final and the slowest step. It is driven

by an electron equivalent transfer from approximately half-reduced low-spin heme *a* and Cu_A to the binuclear center and formation of the fully oxidized state of heme a_3 from the intermediate F (71, 104, 148). During "flow-flash" induced electrometric measurements of the mitochondrial enzyme, two protonic electrogenic phases (~0.7 ms and ~4 ms) coupled to F→O transition has been resolved (103). The τ values and relative amplitudes are in reasonable agreement with the values of 1.2 ms and 4.5 ms found in single electron photoreduction studies (94). Detailed analysis of membrane potential generation combined with parallel optical measurements of the "flow-flash" reaction showed that both A→ P_R→F and F→O generate approximately equal amounts of potential (4, 103, 111, 117).

Bacterial cytochrome oxidases from the A-family. As with mammalian enzyme, the electron injection into F state of the aa_3 oxidases from *R. sphaeroides* (41, 98) or *P.denitrificans* (102) reconstituted into liposomes results in generation of the membrane potential, beginning with the microsecond KCN-insensitive part. This is followed by slower KCN-sensitive portion of the response comprised of two major phases of about equal magnitude if serial sequence of the phases is taken into account (73).

The corresponding charge transfer steps coupled to F→O transition in either *R. sphaeroides* COX (ca. 15 μs, 0.4 ms and 1.5 ms (41, 98)) or *P.denitrificans* oxidase (102) during single-electron reduction measurements are 3-4-fold faster than for the mitochondrial oxidase and have a very similar relative contribution, except of the noticeably higher relative amplitude of the "rapid" electrogenic phase. As shown recently (100), the ~15 μs KCN-insensitive part of charge translocation in bacterial COX is not homogenous and may include an internal proton transfer step (with $\tau \sim 40$ μs) in addition to vectorial electron transfer from Cu_A to heme *a* (with $\tau \sim 10$ μs). The relative contribution of the ~10 μs electrogenic phase, concurring with the optically detected reduction of heme *a* by Cu_A (100, 128) is practically the same as that of the "rapid" electrogenic phase associated with heme *a* reduction in the mitochondrial enzyme (94) and is approximated ~20%. The amplitude of the phase with $\tau \sim 40$ μs is about 2/3 of that of the electron transfer from Cu_A to heme *a.* The intraprotein localization of this minor process remains to be identified. Among other possibilities (100), it might be supposed a shift of proton in the output pathway near Mg^{2+}-binding site, which may be triggered by the electron transfer through Cu_A to the heme *a* (149). As suggested in (149), changes in the redox state of Cu_A may affect ligation state of the Mg^{2+}-binding site. Though it should be kept in mind that fully capable in proton pumping quinol oxidases (like *bo*-oxidase from *E.coli*), do not possess a Cu_A centre.

By applying of the site-directed mutagenesis technique, it was established that electrogenic uptake of both pumped and chemical protons coupled to single-electron photoreduction of the ferryl-oxo state (F→O transition) occurs via the D-channel, while blocking the K-channel does not affect the electrogenic response any significantly (41, 98-100). The D-channel provides all four pumped protons during catalytic cycle (Figure 2) (6, 150-151). The most solid evidence was the findings that site-directed replacement of the amino acid N139D in the D-channel were reported not to pump protons but to retain full or even enhanced catalytic activity (152-153).

The K-channel has been concluded to conduct only the chemical protons during reductive phase of the catalytic cycle, since mutating the K-channel residues blocks the reductive halve of the catalytic cycle and does not affect significantly the oxidative phase (41, 74, 113, 150-151). As was found recently by X-ray structure analysis, the strong hydrogen bonding between hydroxyl of Y288 and the hydroxyethyl farnesyl side chain of heme a_3 may function as a closed gate of the K pathway (30). This bond is present in the oxidized form of COX, prohibiting proton transport via that path to the active site (149), while it is absent in the reduced COX structure in parallel with the appearance of resolved water molecules leading from the top of the K path into the BNC (30).

Time-resolved study of single-electron induced F→O transition in the N139D mutant (COX with uncoupled phenotype) is allowed to calibrate directly the charge transfer coupled to the single-electron transition in the pumping oxidases (99). Initially, the electrogenic distance between Cu_A and heme *a* was estimated as 0.5 of membrane thickness (79, 94-95). It was based on the observation that the shift of apparent midpoint potential of cytochrome *a* (measured as the redox equilibrium between cytochrome *c* and heme *a* in CO inhibited mitochondria at the stationary conditions) corresponds to about half the value of the electric membrane potential imposed (118). The total amplitude of the millisecond protonic electrogenic phases (averaged about ~80% of the photoelectric response for F→O transition) was estimated as transfer of 2 full charges per membrane, which corresponds to uptake into the BNC of one proton during the 0.5 membrane dielectric and additional translocation of about 1.5 pumped protons (79, 94).

Later, this value was reevaluated. It has been found that the total voltage, generated during F→O transition in the uncoupled N139D mutant corresponds to about half that observed with the wild type oxidase (99). As was shown, the ca. 30- 40% of $\Delta\psi$ generation of N139D mutant is coupled to heme *a* reduction step, and ca. 60-70% correspond to proton uptake from the N-phase (99). The contribution of the electron transfer to heme *a* is in close agreement with the value, obtained by theoretical calculations (around 40% in (55)) and matching the geometrical position of Fe ion in heme *a* (around 33% in (26, 119). Assuming the "rapid" electrogenic phase as an electron transfer across ~0.3-0.4 dielectric thickness, the two similar in amplitude protonic electrogenic phases ("intermediate" and "slow") resolved during F→O transition in the wild type and bovine COXs, correspond for each to the H^+ transfer across of about ~ 0.7-0.9 of the dielectric thickness. Uptake of the substrate proton from the N-phase into BNC accounts for transfer across about 0.6-0.7 fraction of membrane, while the resting charge transfer is due to proton pumping. Hence, induced by the single-

electron injection, F→O transition of mammalian and bacterial wild type COXs is coupled to transfer of no more than 1 pumped proton.

Comparative study of the H/D kinetic isotope effects (KIE) of wild type enzyme with N139D mutant proved to be useful solving the question to which proton, pumped or substrate, moves before other during F→O transition. High H/D kinetic isotope effect of the residual protonic phase in N139D matches the KIE measured for the "slow" electrogenic phase in the wild type COX, but it is significantly larger that of the "intermediate" phase (99). Thus the "intermediate" electrogenic phase was found to be missing in the uncoupled mutant. This phase in the wild type oxidase was assigned to translocation of the pumped proton to the situated above the hemes proton-loading site (PLS). Accordingly, the "slow" protonic phase ($\tau \sim 1.5$ ms in wild type) retained by the N139D mutant oxidase was attributed to transfer of the proton required for oxygen chemistry from the inner water phase to the binuclear center (99) and to the extrusion (in case of the wild type enzyme) of the pumped H^+ from PLS to the outside. Similarly, in the "flow-flash" study, the rate of the phase associated with proton release to the output phase was much more sensitive to the H/D kinetic isotope effect (154)

The "intermediate" electrogenic phase is rate-limited by the proton transfer from E286 residue to the PLS, since a single replacement of this residue to aspartate results in the specific delay of the "intermediate" phase (155). The E286 is situated at the intramembrane end of the D-channel at of ca. 15% of the membrane dielectric thickness from the BNC (100). During the F→O transition, this glutamate residue is proposed to be a point of bifurcation, which serves as a donor for intraprotein proton delivery to either the PLS or the binuclear site (156). The single replacement of the glutamate on unprotonatable analog (E286Q) eliminates all proton transfer steps that follow reduction of heme *a* (41).

As was said above, the patterns of charge translocation, coupled to the P_M→F and F→O transitions in the mitochondrial COX and F→O in the bacterial COXs of A-type are very similar. Meanwhile, the ratio of the amplitudes of two protonic electrognic phases, resolved during P_M→F transition of the COX from *R.sphaeroides* looks different from that of F→O of the same species and of the P_M→F and F→O transitions of mitochondrial COX (2.3:1 instead of 1:1.2) (157). Domination of the faster protonic electrogenic phase was observed as well during P_M→F transition of COX from *P.denitrificans* (146). The reasonable suggestion was pointed by M.Verkhovsky (146), which can be used in order to explain this descrepancy. It is based on the possible different channeling of the proton-coupled electron transfer reaction due to difference of the driving forces. As proposed, the electrogenic proton transfer coupled to single-electron transition may occur through the two different regimes, which are characterized by the different (electron or proton transfer) rate-limiting steps. The higher midpoint potential of the electron acceptor (tyrosine radical in the P_M→F) may not only speed up the reaction but also channels it through the way, which does not depend on the rate constant of proton tunneling through the proton-conducting pathway (146) that may eventually result in the apparent acceleration of the "slow" electrogenic component.

The delicate but amazing difference between mitochondrial and bacterial aa_3 cytochrome oxidases of A-family is illustrated by the Figure 3. As shown, the two protonic phases in *R. sphaeroides* COX coupled to the electron transfer from heme *a* to heme a_3 match two phases of heme *a* reoxidation measured by the time resolved optical spectroscopy (Figure 3B, (99-100)). In contrast to the bacterial enzyme, the electrogenic proton transfer in the F→O transition of mitochondrial COX (as well as P_M→F transition (73)) lags behind the electron transfer from heme *a* to the ferryl-oxo complex of a_3 (Figure 3A). The reoxidation of heme *a* occurs in kinetic conjunction with the "intermediate" electrogenic phase, whereas the "slow" electrogenic phase takes place when the electron transfer is essentially over. It is tempting to propose that the part of redox-energy derived from the electron transfer into BNC of the mitochondrial COX is stored in the stretched conformation of the protein matrix, although the more profound study is required probably to clarify the phenomenon.

3.7. O_H→E_H and O→E transitions

For the typical cytochrome *c* oxidases, these transitions can be studied only by single-electron injection method, since the kinetics of oxidation of the fully reduced COX is terminated at the fully oxidized state. As was shown earlier, the initial resting state of the mitochondrial COX and bacterial COX from *P.denitrificans* (O state) is competent neither in the rapid electron transfer into binuclear centre nor in the coupled proton pumping. The single electron injection to the O state gives rise to a single microsecond electrogenic phase matching electron transfer from Cu_A to heme *a* and there is no electron transfer into BNC during the millisecond time region (74, 79-80, 158).

Recently, it was discovered that injection of the electron into the just oxidized state (O_H) of COX from *P. denitrificans,* which is generated upon oxidation of the fully reduced COX by O_2 (74), results in the rapid electron transfer into the Cu_B. This redox centre has transiently high E_m value in the O_H intermediate and serves as a preferred ultimate electron acceptor for the photoinjected electron (75-78). Besides, the electron injection into O_H intermediate of the COX from *P.denitrificans* is coupled to pumping of a proton (74-75).

The four electrogenic phases have been resolved during O_H→E_H transition (75, 146). The first resolved phase ($\tau \sim 10$ μs) has been assigned to the electron transfer from Cu_A to heme *a*, whereas the following three electrogenic phases reflect steps of vectorial proton translocation (75). The net amplitude of the protonic electrogenic steps, associated with the O_H→E_H transition was similar to that coupled to the P_M→F and F→O (74-75). The rate constants of the second (~0.2 ms) and third (~0.8 ms) electrogenic components (75) resemble that of "intermediate" and "slow" phases, associated with F→O

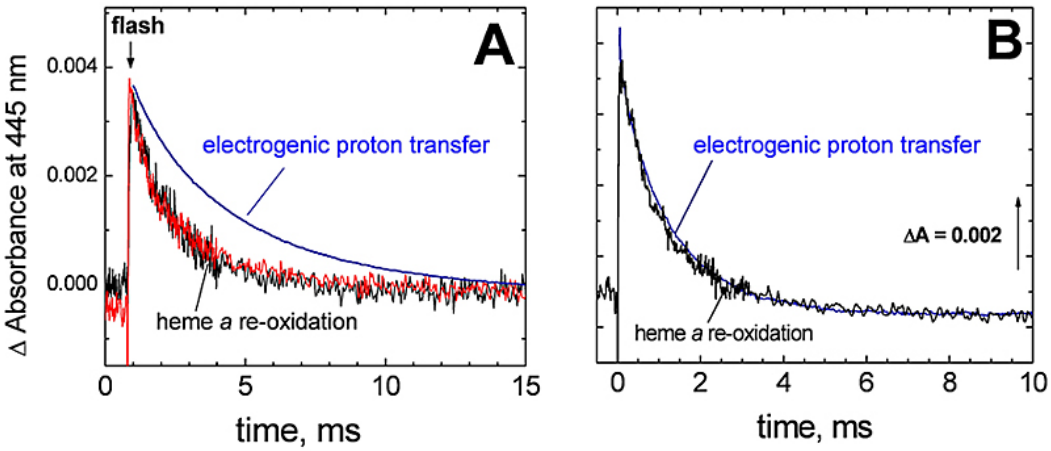

Figure 3. Kinetics of electrogenic proton transfer and heme *a* oxidation in the F→O transition in the mitochondrial (A) and bacterial (B) cytochrome *c* oxidase. The data are given for the F→O transition induced by single electron photoreduction of ferryl-oxo state by RuBpy at pH 8. (A) In the mitochondrial oxidase, KCN-sensitive electrogenic proton transfer (blue curve) lags behind reoxidation of the photoreduced heme *a* measured at 445 nm in either solubilized (black curve) or liposome-reconstituted COX (red curve) (122, 174). (B) In the cytochrome oxidase from *R. sphaeroides*, KCN-sensitive electrogenic proton transfer matches kinetically reoxidation of heme *a* (99-100). For experimental details, see refs. (99, 174).

transition of the COXs from *P.denitrificans* and *R.sphaeroides* (99, 102). The relative amplitudes of these phases are in agreement with their attribution to uptake of pumped proton from the N-phase to the PLS and chemical proton to the BNC, correspondingly (55, 75). The forth electrogenic component ($\tau \sim 2.6$-5.3 ms) was attributed to the slow release of the proton from the PLS (75).

In contrast to $P_M \rightarrow F$ and $F \rightarrow O$ transitions, during the $O_H \rightarrow E_H$ transition only the pumped proton is transferred through the D-pathway, whereas the substrate proton is taken from the protonic K-channel (74). The K-pathway is opened in the reductive halve of the catalytic cycle, while it is proposed to be closed during oxidative half by the hydrogen bonding between hydroxyl of Y288 and the hydroxyethyl farnesyl side chain of heme a_3, functioning as a proton gate (30).

3.8. E→R transition

Addition of a second electron to E_H state creates a two-electron reduced form of enzyme. Starting from the fully reduced state of COX, the oxidative and reductive halves of the catalytic cycle were concluded to be approximately equivalent in relative to the transmembrane potential generation (120). Assuming that $O_H \rightarrow E_H$, $F \rightarrow O$ and $P_M \rightarrow F$ are coupled to pumping of approximately 1 proton, the resting forth pumped proton should be associated with the $E_H \rightarrow R$ transition (Figure 2) (4).

However, $E_H \rightarrow R$ transition is the least explored with a time resolution and consequently less understood step of the catalytic cycle. Being produced from the O_H state, the E_H was not studied directly by the single-electron reduction approach, because of difficulties with stabilization of the COX in this state. A state of enzyme bearing under special conditions about one, on the average, electron equivalent was checked by the single-electron injection technique and the kinetics of membrane potential generation was similar to that of the F→O transition (102). However, in this case the electron equivalent was distributed among heme *a*, heme a_3 and Cu_B (102), whereas in the E_H state, formed by electron injection into the O_H state the electron locates exclusively on the Cu_B (75, 77-78). On the other hand, analysis of multiple electron injection into the O state of COX suggest the electron injection into enzyme molecules with the one-electron reduced state of BNC is only accompanied by the electrogenic uptake of substrate proton through the K-channel and is not competent in proton pumping (80). More experiments are necessary to shed light on these discrepancies.

4. SEQUENCE OF THE EVENTS DURING TRANSFER OF THE 4th ELECTRON IN CATALYTIC CYCLE

From the theoretical considerations, the redox-driven pump must contain at least one site ("pumping element") which should be passed from time to time through the contact with the inner and the outer surface of the protein and in so doing it should never be accessible to protons from both of the protein surfaces simultaneously. Besides, the pumping element should change its protonation state, depending on the redox state of the active site and state of the gating mechanism that needs to provide a directionality of the proton transfer to the outer phase and to inhibit a pump proton from dropping back (8, 54, 159). In the most current models of cytochrome oxidase, the pumping element is associated primarily with the PLS, located above heme centres (11, 54, 99, 160).

There is growing evidence (see above) that each of the four 1-electron transfers to the active site of cytochrome *c* oxidase during the reduction of O_2 to H_2O results in the net transfer of two elementary charges across the membrane (74-75, 79, 94, 99, 102-103, 105, 120-121).

One charge is associated with the chemistry and the second charge due to the pumping of one proton. It is significant that the two-component patterns of the electrogenic events, reflecting vectorial proton transfer coupled to the single-electron reduction of BNC were resolved for the F→O, P_M→F and O_H→E_H transitions (74, 79, 94, 99, 102-104, 113, 120). In addition, the two electrogenic stages, linked to the reaction sequence of A→P_R→F were assigned recently to the two sequential processes of the proton transfer, coupled to the single-electron transfer from heme *a* to the BNC during A→P_R (111).

The two similar in amplitude protonic electrogenic phases, coupled to F→O transition (41, 73, 99, 103-104) can be reasonable assigned to the consecutive proton transfer from the inner water phase to the PLS and BNC, contaminated with other minor electrogenic events. Study of the uncoupled N139D mutant shows that protonation of the PLS occurs through the "intermediate" electrogenic phase, whereas the selective deceleration by the Zn^{2+} from the output phase indicates that the "slow" electrogenic phase is associated with release of the pumped proton to the P-side of the membrane.

Figure 4 shows schematically the sequence of the events coupled to F→O transition. During the first protonic electrogenic component, there should be the electrogenic proton transfer of the pumped proton to the PLS from E286 which is accompanied by immediate re-protonation of E286 from the N-phase (steps 2 and 4, Figure 4). The first step of proton translocation (to the PLS) is followed by the second resolved electrogenic component, which includes ejection of the pumped proton from the PLS (step 7, Figure 4) and the electrogenic uptake from N-phase of a second proton to the E286 (step 6, Figure 4) or to the BNC. There is uncertainty on to which of electrogenic components, the substrate proton transfer from E286 to the BNC (step 5, Figure 4) should be included (73). This subject is closely related to the two ways of the coupling between proton pumping and oxygen reduction site change, which can be suggested.

In general, the coupling may be purely electrostatic or it can be controlled by change of conformation of the protein. According to the basic electrostatic mechanism (11, 67, 123), reduction of the heme *a* raises pK_a of PLS and induces a proton transfer from the inner water phase through E286 to the PLS (steps 2 and 4, Figure 4). A proton delivery to the PLS in turn triggers electron equilibration between hemes by raising redox-potential of the BNC and allowing electron transfer from heme *a*, which occurs with the same kinetics as loading of the PLS (step 3, Figure 4) (11, 75, 123). Another modification of this mechanism predicts that it is a transfer of an electron from heme *a* to the binuclear centre, which is then followed by proton delivery to the pump site (54). As a consequence of the BNC reduction, a substrate proton is taken up from the N-side into BNC and this expels the pumped proton from the PLS into the P-side by electrostatic repulsion (steps 6 and 7, Figure 4). This sequence of events was originally brought to explain the time-resolved O_H→E_H transition, where the first protonic electrogenic phase (~150 μs) was attributed to proton delivery to the PLS from the N-phase during D-channel concurrently with electron transfer from heme *a* to the heme a_3. The second protonic electrogenic phase (~800 μs) was assigned to proton transfer into the BNC through the protonic K-channel coupled to the electron redistribution from heme a_3 to the Cu_B (11, 75).

This mechanism predicts for the proton transfer to BNC is preceded by the proton delivery to the PLS. Since during oxidative half of the catalytic cycle, the D-channel provides a proton also to the BNC, it is proposed that initial protonation of PLS can be more favorable thermodynamically (67) or it can be faster than delivery of proton to the BNC because of the more loose structure of water array forming the latter pathway within a nonpolar cavity beyond E286 residue (49, 52, 54). As captured by BNC, the electron attracts a "chemical" proton by the electric fields, polarizing functional water molecules in the direction to the BNC (123). A control of the back-leakage of the pumped proton from the PLS to E286 residue can be provided by the conformational change of the E286, acting as a valve in the proton-pumping mechanism (step 1, Figure 4) (161).

This model can be applied with some assumptions to the F→O transition in bacterial COX from *R.sphaeroides*. During F→O transition, both substrate and pumped protons are provided exclusively by the D-channel and the final electron acceptor is a heme a_3. The protonic, KCN-sensitive part of the kinetics of membrane potential generation in *R. sphaeroides* COX match roughly the kinetics of heme *a* reoxidation measured spectrophotometrically and two components with similar relative constants and apparent amplitudes were resolved for both of electrometric and optical measurements (100). That is, the main part of the optical changes (~70%, (100)) occurs through the slowest phase. More of that, taking into consideration that the electrometric phases needs to be recalculated due to consecutive scheme, the kinetics of optical changes due to heme *a* reoxidation should be lags behind the recalculated voltage changes and the larger amplitude of the slowest phase of the optical changes may indicate the process of electron transfer and proton delivery to the BNC proceed concurrently with the "slow" electrogenic phase. If substrate proton is to be delivered to the BNC during the "slow" electrogenic phase, then the minor optical changes matching the "intermediate" electrogenic phase of aa_3 oxidase from *R.sphaeroides* may indicate a shift of electron density to the BNC in response to protonation of the PLS.

Meanwhile, the application of this mechanism to the mitochondrial COX meets a problem, arising from the mentioned above, evident retardation of the protonic electrogenic transfer as compared to the coupled electron reduction of BNC. It being shown that the reoxidation of heme *a* of the mitochondrial enzyme occurs in kinetic conjunction with the "intermediate" electrogenic phase, whereas the "slow" electrogenic phase takes place when the

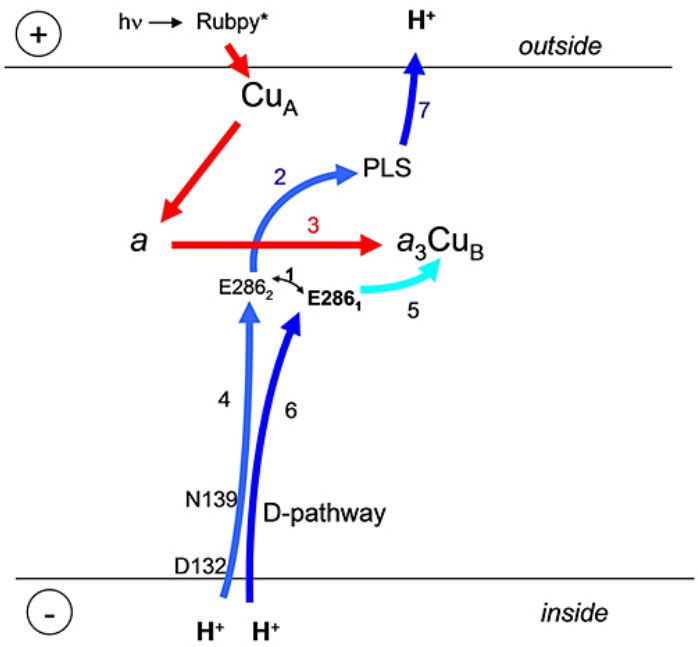

Figure 4. Electrogenic steps coupled to transfer of the 4th electron in cytochrome oxidase. The scheme shows major partial electrogenic steps resolved by single-electron photoreduction experiments for the F→O transition. Although not depicted, heme a_3 is meant to be in the ferryl-oxo state prior to the flash pulse. Major electrogenic steps are denoted by the arrows*: red arrows*, electron transfer; *blue arrows*, substrate and pumped protons. During the F→O step, both the pumped and chemical protons are delivered via the D-channel. The partial steps 2, 3 and 4 merge to form electrogenic protonic "intermediate" phase, and the steps 6 and 7 merge in electrogenic protonic "slow" phase. The partial step 5 is proposed to be included into the "slow" phase in the COX from *R. sphaeroides* or into the "intermediate" protonic phase in the mitochondrial enzyme. According to the structural data (29), two possible conformation states ($E286_1$ and $E286_2$) of the E286 residue are displayed. It is suggested that the isomerization of the E286 (step 1) proceeds the proton transfer to the PLS (step 2). Following (165), the E286 residue is proposed to be able to donate proton to the BNC or to the PLS in the different conformational states ($E286_1$ and $E286_2$, correspondingly). Noticeably, the another point of view suggest that the same conformational state of the E286 residue may serve as a donor of proton for both of BNC and PLS, while the isomerization of E286 side chain is needed to reconnect this residue to the top of D-channel for their reprotonation from the bulk phase (161, 172).

electron transfer is essentially over. In this case, there is uncertainty with an immediate donor of substrate proton during the "intermediate" phase (122). If E286 residue, the most prominent candidate, donates both pumped and substrate protons during "intermediate" electrogenic phase, it should retain the anionic form up to re-protonation during the "slow" phase. Though recent experiments indicates the transient unprotonated form of the E286 residue through the turnover of the mutant with blocked entrance to the D-channel (126), the possibility of this state in the native enzyme is under matter of controversies due to energetically favorable immediate re-protonation of the E286 via the D-channel (162).

Noticeably, if the chemical proton is delivered to BNC during the "intermediate" electrogenic phase, it must be linked to the structural change that conserves a substantial part of the free energy, released later during the "slow" electrogenic phase. This rather implies another type of the coupling between proton pumping and oxygen reduction site which is based on the conformation controlling (127, 160, 163-164).

In spite of the available structures of the oxidized and reduced forms of COX appear to be very similar, several models were proposed that involve structural changes in COX during proton pumping. A mechanism, based upon structural data indicating conformational isomerization and deprotonation of E286 residue linked to perturbation in area of the heme propionates of COX from *R.sphaeroides* (29), was suggested by Brzezinki and Larsen (127, 160). As proposed, the chemical proton transfer from E286 to the BNC occurs first (step 5, Figure 4). The deprotonated E286 residue shifts upward toward a cluster of heme *a* and a_3 propionate groups (step 1, Figure 4) that leads to a conformationally strained state with a substantial increased the proton affinity of PLS (f.e. by the negative charge of the deprotonated E286) that secondarily drive the pumped proton to the PLS (step 2 and 4, Figure 4) (127, 160, 165). After that, reprotonation of E286 from the inner surface allows it to relax to its original position, resulting in a drop of the pK_a of the accepting cluster, and the proton is ejected to the positive surface of the membrane (steps 6 and 7, Figure 4).

Based on the molecular dynamics simulations of COX from *R.sphaeroides*, another proton pumping mechanism, involving structural changes at a distance from the active site was suggested (166). It supposes the key role of movement of the conserved loop of COX, bringing W172 residue within hydrogen-bonding distance of E286 providing proton transfer from E286 to a heme a_3 propionate (166). The structural changes during pump cycle of COX, induced by the dissociation of the Cu_B ligands (H334 residue or H284-Y288 cross-linked pair) in response to the overall charge at the heme a_3-Cu_B center were suggested in models, described in (149, 167). By way of example, the "intermediate" electrogenic phase of mammalian COX could be associated with dissociation of the Cu_B ligand linked to the reduction of BNC and with generation of the non-equilibrium state of the protein surroundings around the binuclear site, releasing the energy through the "slow" electrogenic phase.

Finally, based on the structural analysis of the mitochondrial COX, the mechanism was deduced, which implies the role of an alternative proton-conductive H-pathway in translocation of pumped protons from N- to the P-side of the membrane (163-164). It is suggested that heme *a* is a driving element of proton pump (9). The putative H-channel passes near the formyl group of heme *a* to the D51 residue, situated at the top of the H-pathway. As proposed from the X-ray data, the aspartate 51 changes its conformation depending on the reduction state of heme *a* providing the gate for proton translocation through the membrane (163-164). The application of this mechanism is complicated however, by the fact that no electrogenic uptake of proton, coupled to the heme *a* reduction was found during time-resolved single-electron injection study of the bovine COX so far. Besides, it is noted, the mitochondrial and A-family bacterial COXs mechanisms are suggested to be very similar, whereas this structural change can be strict exclusively to the mammalian enzyme, since the key residues of H-channel are not conserved in the bacterial COXs (4, 6, 11).

So, despite of the similarity between different representatives of the A family, the unified electrogenic mechanism can not explain to date all set of experimental electrogenic results for the each one-electron transition.

5. PECULIARITIES OF THE ba_3 CYTOCHROME OXIDASE FROM *THERMUS THERMOPHILUS*

The ba_3 cytochrome oxidase from *Thermus thermophilus* belongs to the B family of heme-copper oxidases and differs in several important respects from the A-family representatives (12-13). Although cytochrome ba_3 lacks most of the highly conserved amino acid residues that form input proton channels in the A-family oxidases, it nevertheless generates an electric transmembrane potential difference under steady-state conditions, and pumps protons with twice lower efficiency (H^+/e^- ~ 0.5) (115, 168). Of the three potential proton channels resolved in structure of cytochrome ba_3, there is compelling evidence only for the K-channel homologue being involved in the enzyme functioning (14).

In contrast to the O state of typical aa_3 cytochrome oxidases, the 1st electron photoinjected into the oxidized resting state of ba_3 oxidase goes rapidly to the binuclear site, equilibrating between the hemes *b* and a_3 at the ratio of 2.3:1 (77). Under these conditions, the KCN-insensitive electrogenic phase of electron transfer from Cu_A to heme *b* (τ ~ 20 μs) is followed by partial electron transfer from heme *b* to the binuclear site coupled to electrogenic proton transfer with τ of ~0.25 ms (169). Taking to account the extent of electron redistribution between heme *b* and heme a_3, the magnitude of the 0.25 ms electrogenic phase is about 2.2 that of the rapid KCN-insensitive phase. Presumably, the single electron reduction of the oxidized (O state) ba_3 is coupled to proton uptake from the N-phase via the K-channel associated with electron transfer to heme a_3 (131) but not to proton pumping.

Like non-relaxed oxidized O_H state of aa_3 cytochrome oxidase from *P. denitrificans,* the "activated" oxidized state (O_H) of cytochrome ba_3 is fully competent in rapid electron transfer from the input redox-centers into the catalytic heme-copper site (77). However, the rate of electron transfer to heme a_3 during $O_H \rightarrow E_H$ transition of ba_3 cytochrome oxidase from *T. thermophilus* is as fast (τ ~ 17 μs) as that from Cu_A to the low spin heme (77). This is in significant contrast to the $O_H \rightarrow E_H$ transition of the aa_3-type cytochrome oxidase, where the fastest phase is exclusively due to transient reduction of the low-spin heme *a*, without electron equilibration with the binuclear center (75). It is still unknown whether the $O_H \rightarrow E_H$ transition in the ba_3 enzyme is capable of proton pumping across the membrane, as was found earlier for *P. denitrificans* aa_3 oxidase (75).

Time-resolved electrometric studies on the oxidation of the fully-reduced COX by molecular oxygen in the single-turnover regime (115) shows that F→O step of ba_3 cytochrome oxidase from *T. thermophilus* is likely to retain normal capability to the coupled transfer of 2 charges across the membrane, while stage of the compound F formation is twice less electrogenic and, hence, is likely to slip the proton pumping. Besides, the F state in cytochrome ba_3 has a spectrum identical to the P_R state, which indicates that the proton taken up during $P_R \rightarrow F$ transition does not reside in the binuclear site but is rather transferred to the covalently cross-linked tyrosine near the site (115).

In the oxidized resting state (O), the binuclear centre of ba_3 oxidase from *T. thermophilus* is closed and reacts very slowly with any of the heme a_3 ligands tested, including H_2O_2 (169). Therefore the charge transfer events coupled to the 3-rd and 4-th electrons in catalytic cycle of this enzyme were not investigated in detailes by the single-electron injection technique. The electron transfer reaction of ba_3 COX, which may be in part viewed as an analog of the P→F transition in aa_3 cytochrome oxidases, can be induced by single-electron injection in presence of peroxide (169). Photoinjection of a single electron into the oxidized enzyme opens the binuclear site for rapid interaction with exogenous H_2O_2 that was revealed by appearance of the

additional electrogenic phase, rate of which depends linearly on H_2O_2 concentration (169). As a result, the membrane potential generation coupled to single-electron photoreduction of ba_3 in presence of H_2O_2 includes 3 phases with $\tau_1 \sim 20$ μs (r.a. ~ 31%); $\tau_2 \sim 0.42$ ms (r.a. ~ 23%) and additional 3rd phase with $\tau_3 \sim 11.6$ ms (at 40 mM H_2O_2; r.a. ~ 46%) (169). The first rapid phase is KCN-insensitive and is linked to reduction of the low-spin heme *b*. The 2nd and 3rd phases are fully prevented by KCN and are coupled to the electron transfer from heme *b* to the binuclear site, reducing the bound H_2O_2 molecule.

The magnitude ratio of phases associated with the reduction and reoxidation of the low-spin heme *b* attains a value of 1:2.2 that is consistent with proposition that the P→F transition is not coupled to pumping of a proton (115). A provisional conclusion is that in ba_3 oxidase, the O→E and $P_{R(M)}$→F single-electron steps are not coupled to the transmembrane proton translocation, whereas the F→O and probably E_H→R transitions are fully capable in proton pumping. This is in agreement with a recent proposal (170), suggesting the pump site in ba_3 cytochrome oxidase may alternate between a protonated and deprotonated state for every second electron transferred to the catalytic site.

6. PERSPECTIVES

There has been significant progress in understanding the functional properties of cytochrome oxidase due to the determination of their crystallographic structure with high resolution, functional studies using biophysical techniques, and theoretical calculations. However, a lot of questions on structure-functional relationships in COX remain to be answered. It is not known with accuracy what is a proton pump site. The structural features of the so-called "activated" states, O_H and E_H are still unknown. More efforts are needed to explain the uncoupling effect in the mutants with lost proton pumping ability (171) and to resolve the molecular nature of gating of the proton pump mechanism, providing a directionality of the proton transfer and inhibiting a pump proton backflow due to electrochemical gradient (161, 172). Role of the H-pathway, described in mitochondrial COX, is unclear in the bacterial oxidases and this is also for the advantage of particular using of the protonic D and K channels during oxidative and reductive halves of the catalytic cycle.

Time-resolved studies of the charge transfer events during catalytic cycle of cytochrome oxidase revealed many similar things in the electrogenic mechanism of different heme-coper cytochrome oxidases, especially between eukaryotic COX and homologous bacterial COXs from the A-family. Meanwhile, there are distinctions in the electrogenic behavior, which may indicate the principal differences in the electrogenic mechanism between COXs from the different species. Despite of a number of models proposed, it is still not known in details how the rate and direction of proton movement is controlled and coordinated to electron transfer in the all different steps of catalytic cycle of COX, which is required to propose a unified molecular mechanism of coupling.

There are many parallels in mechanisms of cytochrome oxidase and photosystem II, molecular mashines, which play a key role in the pathways of consumption and creation of dioxygen in living systems. Both of enzymes are the highly efficient energy transducers that generate a membrane potential difference by coupling of the four consecutive single electron transitions of the catalytic site to transmembrane charge translocation. Among other things, the fascinating similarities between these enzymes include significant role of tyrosine residue in the catalytic cycle, described for both mechanisms, and the special pathways for intraprotein translocation of protons, dioxygen and water. Hence, a comparative study of the electrogenic mechanisms in these enzymes may be mutually useful.

7. ACKNOWLEDGMENTS

The work has been supported by the grants from Russian Fund for Basic Research (06-04-48608 and 09-04-00140 to S.A.S).

8. REFERENCES

1. Anraku, Y.: Bacterial electron transport chains. *Ann Rev Biochem*, 57, 101-132 (1988)

2. Garcia-Horsman, J. A., B. Barquera, J. Rumbley, J. Ma & R. B. Gennis: The superfamily of heme-copper respiratory oxidases. *J Bacteriol*, 176, 5587-5600 (1994)

3. Ferguson-Miller, S. & G. T. Babcock: Heme/copper terminal oxidases. *Chem Rev*, 7, 2889-2907 (1996)

4. Belevich, I. & M. I. Verkhovsky: Molecular mechanism of proton translocation by cytochrome *c* oxidase. *Antioxidants and Redox Signaling*, 10, 1-29 (2008)

5. Pereira, M. M., M. Santana & M. Teixeira: A novel scenario for the evolution of haem-copper oxygen reductases**.** *Biochim Biophys Acta*, 1505, 185-208 (2001)

6. Brzezinski, P. & R. B. Gennis: Cytochrome c oxidase: exciting progress and remaining mysteries. *J Bioenerg Biomembr*, 40, 521-531 (2008)

7. Brzezinski, P. & A. L. Johansson: Variable proton-pumping stoichiometry in structural variants of cytochrome c oxidase. *Biochim Biophys Acta*, 1797, 710-23 (2010)

8. Hosler, J. P., S. Ferguson-Miller & D. A. Mills: Energy transduction: proton transfer through the respiratory complexes. *Annu Rev Biochem*, 75, 165-187 (2006)

9. Yoshikawa, S., K. Muramoto & K. Shinzawa-Itoh: Proton-pumping mechanism of cytochrome *c* oxidase. *Annu Rev Biophys*, 40, 205-23 (2011)

10. Rich, P. R. & A. Marechal: The mitochondrial respiratory chain. *Essays Biochem*, 47, 1-23 (2010)

11. Wikstrom, M. & M. I. Verkhovsky: Mechanism and energetics of proton translocation by the respiratory heme-copper oxidases. *Biochim Biophys Acta*, 1767, 1200-1214 (2007)

12. Zimmermann, B. H., C. I. Nitsche, J. A. Fee, F. Rusnak & E. Munck: Properties of a copper-containing cytochrome ba_3: a second terminal oxidase from the extreme thermophile *Thermus Thermophilus*. *Proc Natl Acad Sci USA*, 85, 5779-5783 (1988)

13. Soulimane, T., G. Buse, G. B. Bourenkov, H. D. Bartunik, R. Huber & M. E. Than: Structure and mechanism of the aberrant ba_3-cytochrome *c* oxidase from *Thermus thermophilus*. *EMBO J*, 19, 1766-1776 (2000)

14. Chang, H. Y., J. Hemp, Y. Chen, J. A. Fee & R. B. Gennis: The cytochrome ba_3 oxygen reductase from *Thermus thermophilus* uses a single input channel for proton delivery to the active site and for proton pumping. *Proc Natl Acad Sci U S A*, 106, 16169-73 (2009)

15. Pitcher, R. S. & N. J. Watmough: The bacterial cytochrome cbb_3 oxidases. *Biochim Biophys Acta*, 1655, 388-99 (2004)

16. Rauhamaki, V., D. A. Bloch, M. I. Verkhovsky & M. Wikstrom: Active site of cytochrome cbb_3. *J. Biol. Chem.*, 284, 11301-11308 (2009)

17. Buschmann, S., E. Warkentin, H. Xie, J. D. Langer, U. Ermler & H. Michel: The structure of cbb_3 cytochrome oxidase provides insights into proton pumping. *Science*, 329, 327-30 (2010)

18. Hemp, J. & R. B. Gennis: Diversity of the heme-copper superfamily in archaea: insights from genomics and structural modeling. *Results Probl Cell Differ*, 45, 1-31 (2008)

19. Mitchell, P.: Chemiosmotic coupling and energy transduction. Glynn Research Ltd., Bodmin (1968)

20. Wikstrom, M.: Proton pump coupled to cytochrome *c* oxidase in mitochondria. *Nature*, 266, 271-273 (1977)

21. Wikstrom, M.: Cytochrome c oxidase: 25 years of the elusive proton pump. *Biochim Biophys Acta*, 1655, 241-247 (2004)

22. Tsukihara, T., H. Aoyama, E. Yamashita, T. Takashi, H. Yamaguichi, K. Shinzawa-Itoh, R. Nakashima, R. Yaono & S. Yoshikawa: The whole structure of the 13-subunit oxidized cytochrome c oxidase at 2.8 A. *Science*, 272, 1136-1144 (1996)

23. Yoshikawa, S., K. Shinzawa-Itoh, R. Nakashima, R. Yaono, N. Inoue, M. Yao, M. J. Fei, C. P. Libeu, T. Mizushima, H. Yamaguchi, T. Tomizaki & T. Tsukihara: Redox-coupled crystal structural changes in bovine heart cytochrome *c* oxidase. *Science*, 280, 1723-1729 (1998)

24. Tsukihara, T., K. Shimokata, Y. Katayama, H. Shimada, K. Muramoto, H. Aoyama, M. Mochizuki, K. Shinzawa-Itoh, E. Yamashita, M. Yao, Y. Ishimura & S. Yoshikawa: The low-spin heme of cytochrome *c* oxidase as the driving element of the proton-pumping process. *Proc Natl Acad Sci USA*, 100, 15304-15309 (2003)

25. Muramoto, K., K. Hirata, K. Shinzawa-Itoh, S. Yoko-o, E. Yamashita, H. Aoyama, T. Tsukihara & S. Yoshikawa: A histidine residue acting as a controlling site for dioxygen reduction and proton pumping by cytochrome *c* oxidase. *Proc Natl Acad Sci USA*, 104, 7881-7886 (2007)

26. Iwata, S., C. Ostermeier, B. Ludwig & H. Michel: Structure at 2.8 A resolution of cytochrome *c* oxidase from *Paracoccus denitrificans*. *Nature*, 376, 660-669 (1995)

27. Ostermeier, C., S. Iwata, B. Ludwig & H. Michel: FV fragment-mediated crystallization of the membrane protein bacterial cytochrome *c* oxidase. *Nat Struct Biol*, 2, 842 (1995)

28. Koepke, J., E. Olkhova, H. Angerer, H. Muller, G. Peng & H. Michel: High resolution crystal structure of *Paracoccus denitrificans* cytochrome *c* oxidase: New insights into the active site and the proton transfer pathways. *Biochim Biophys Acta*, 1787, 635-645 (2009)

29. Svensson-Ek, M., J. Abramson, G. Larsson, S. Tornroth, P. Brzezinski & S. Iwata: The X-ray crystal structures of wild-type and EQ(I-286) mutant cytochrome *c* oxidases from *Rhodobacter sphaeroides*. *J Mol Biol*, 321, 329-339 (2002)

30. Qin, L., J. Liu, D. A. Mills, D. A. Proshlyakov, C. Hiser & S. Ferguson-Miller: Redox dependent conformational changes in cytochrome *c* oxidase suggest a gating mechanism for proton uptake. *BIochemistry*, 48, 5121-5130 (2009)

31. Abramson, J., S. Riistama, G. Larsson, A. Jasaitis, M. Svensson-Ek, L. Laakkonen, A. Puuustinen, S. Iwata & Wikstrom: The structure of the ubiquinol oxidase from *Escherichia coli* and its ubiquinone binding site. *Nat Struct Biol*, 7, 910-917 (2000)

32. Luna, V. M., Y. Chen, J. A. Fee & C. D. Stout: Crystallographic studies of Xe and Kr binding within the large internal cavity of cytochrome *ba*3 from *Thermus thermophilus*: Structural analysis and role of oxygen transport channels in the heme-Cu oxidases. *Biochemistry*, 47, 4657-4665 (2008)

33. Pilet, E., A. Jasaitis, U. Liebl & M. H. Vos: Electron transfer between hemes in mammalian

cytochrome *c* oxidase. *Proc Natl Acad Sci USA*, 101, 16196-16203 (2004)

34. Buse, G., T. Soulimane, M. Dewor, H. E. Meyer & M. Bloggel: Evidence for a copper coordinated histidine-tyrosine crosslink in the active site of cytochrome oxidase. *Protein Sci*, 8, 985-990 (1999)

35. Rauhamaki, V., M. Baumann, R. Soliymani, A. Puustinen & M. Wikstrom: Identification of histidin-tyrosin cross-link in the active site of the cbb_3-type cytochrome *c* oxidase from *Rhodobacter sphaeroides*. *Proc Natl Acad Sci U S A*, 103, 16135-16140 (2006)

36. Babcock, G. T.: How oxygen is activated and reduced in respiration. *Proc Natl Acad Sci USA*, 96, 12971-12973 (1999)

37. Proshlyakov, D. A., M. A. Pressler, C. DeMaso, J. F. Leykam, D. L. DeWitt & G. L. Babcock: Oxygen activation and reduction in respiration: involvement of redox-active tyrosine 244. *Science*, 290, 1588-1591 (2000)

38. Gennis, R. B.: Coupled proton and electron transfer reactions in cytochrome oxidase. *Front Biosci*, 9, 581-91 (2004)

39. Mills, D. A. & J. P. Hosler: Slow proton transfer through the pathways for pumped protons in cytochrome *c* oxidase induces suicide inactivation of the enzyme. *Biochemistry*, 44, 4556-4666 (2005)

40. Fetter, J. R., J. Qian, J. Shapleigh, J. W. Thomas, A. Garcia-Horsman, E. Schmidt, J. Hosler, G. T. Babcock, R. B. Gennis & S. Ferguson-Miller: Possible proton relay pathways in cytochrome *c* oxidase. *Proc Natl Acad Sci USA*, 92, 1604-1608 (1995)

41. Konstantinov, A. A., S. Siletsky, D. Mitchell, A. Kaulen & R. B. Gennis: The roles of the two proton input channels in cytochrome *c* oxidase from *Rhodobacter sphaeroides* probed by the effects of site-directed mutations on time resolved electrogenic intraprotein proton transfer. *Proc Natl Acad Sci USA*, 94, 9085-9090 (1997)

42. Gennis, R. B.: Multiple proton-conducting pathways in cytochrome oxidase and a proposed role for the active-site tyrosine. *Biochim Biophys Acta*, 1365, 241-248 (1998)

43. Qin, L., C. Hiser, A. Mulichak, R. M. Garavito & S. Ferguson-Miller: Identification of conserved lipid/detergent-binding sites in a high-resolution structure of the membrane protein cytochrome *c* oxidase. *Proc Natl Acad Sci U S A*, 103, 16117-16122 (2006)

44. Branden, M., F. Tomson, R. B. Gennis & P. Brzezinski: The entry point of the K-proton-transfer pathway in cytochrome *c* oxidase. *Biochemistry*, 41, 10794-10798 (2002)

45. Hofacker, I. & K. Schulten: Oxygen and proton pathways in cytochrome *c* oxidase. *Proteins*, 30, 100-107 (1998)

46. Shimokata, K., Y. Katayama, H. Murayama, M. Suematsu, T. Tsukihara, K. Muramoto, H. Aoyama, S. Yoshikawa & H. Shimada: The proton pumping pathway of bovine heart cytochrome *c* oxidase. *Proc Natl Acad Sci U S A*, 104, 4200-4205 (2007)

47. Pfitzner, U., A. Odenwald, O. T.., L. Weingard, B. Ludwig & O. M. Richter: Cytochrome *c* oxidase (heme aa_3) from *Paracoccus denitrificans*: analysis of mutations in putative proton channels of subunit I. *J Bioenerg Biomembr*, 30, 89-97 (1998)

48. Lee, H.M., T. K. Das, D. L. Rousseau, D. Mills, S. Fergusson-Miller & R. Gennis: Mutations in the putative H-channel in the cytochrome *c* oxidase from *Rhodobacter sphaeroides* show that this channel is not important for proton conduction but reveals modulation of the properties of heme *a*. *Biochemistry*, 39, 2989-2996 (2000)

49. Wikstrom, M., M. I. Verkhovsky & G. Hummer: Water-gated mechanism of proton translocation by cytochrome *c* oxidase. *Biochim Biophys Acta*, 45238, 1-5 (2003)

50. Cukier, R. I.: Quantum molecular dynamics simulation of proton transfer in cytochrome *c* oxidase. *Biochim Biophys Acta*, 1656, 189-202 (2004)

51. Tashiro, M. & A. A. Stuchebrukhov: Thermodynamic properties of internal water molecules in the hydrophobic cavity around the catalytic center of cytochrome *c* oxidase. *J Phys Chem B*, 109, 1015-22 (2005)

52. Zheng, X., D. M. Medvedev, J. Swanson & A. A. Stuchebrukhov: Computer simulation of water in cytochrome *c* oxidase. *Biochim Biophys Acta*, 1557, 99-107 (2003)

53. Michel, H.: Cytochrome *c* oxidase: catalytic cycle and mechanisms of proton pumping - a discussion. *Biochemistry*, 38, 15129-40 (1999)

54. Popovic, D. M. & A. A. Stuchebryukhov: Proton pumping mechanism and catalytic cycle of cytochrome *c* oxidase: Coulomb pump model with kinetic gating. *FEBS Lett.*, 566, 126-130 (2004)

55. Sugitani, R., E. S. Medvedev & A. A. Stuchebrukhov: Theoretical and computational analysis of the membrane potential generated by cytochrome *c* oxidase upon single electron injection into the enzyme. *Biochim Biophys Acta*, 1777, 1129-39 (2008)

56. Kaila, V. R., V. Sharma & M. Wikstrom: The identity of the transient proton loading site of the proton-pumping mechanism of cytochrome c oxidase. *Biochim Biophys Acta*, 1807, 80-4 (2011)

57. Popovic, D. M. & A. A. Stuchebrukhov: Proton exit channels in bovine cytochrome c oxidase. *J Phys Chem B*, 109, 1999-2006 (2005)

58. Riistama, S., A. Puustinen, M. I. Verkhovsky, J. E. Morgan & M. Wikstrom: Binding of O2 and its reduction are both retarded by replacement of valine 279 by isoleucine in cytochrome c oxidase from Paracoccus denitrificans. *Biochemistry*, 39, 6365-72 (2000)

59. Salomonsson, L., A. Lee, R. B. Gennis & P. Brzezinski: A single-amino-acid lid renders a gas-tight compartment within a membrane-bound transporter. *Proc Natl Acad Sci* U S A, 101, 11617-21 (2004)

60. Sugitani, R. & A. A. Stuchebrukhov: Molecular dynamics simulation of water in cytochrome c oxidase reveals two water exit pathways and the mechanism of transport. *Biochim Biophys Acta*, 1787, 1140-1150 (2009)

61. Schmidt, B., J. McCracken & S. Ferguson-Miller: A discrete water exit pathway in the membrane protein cytochrome *c* oxidase. *Proc Natl Acad Sci USA*, 100, 15539-15542 (2003)

62. Hill, B. C. & C. Greenwood: Spectroscopic evidence for the participation of compound A (Fea_3^{2+}-O_2) in the reaction of mixed-valence cytochrome *c* oxidase with oxygen at room temperature. *Biochem J*, 215, 659-67 (1983)

63. Muramoto, K., K. Ohta, K. Shinzawa-Itoh, K. Kanda, M. Taniguchi, H. Nabekura, E. Yamashita, T. Tsukihara & S. Yoshikawa: Bovine cytochrome *c* oxidase structures enable O_2 reduction with minimization of reactive oxygens and provide a proton-pumping gate. *Proc Natl Acad Sci U S A*, 107, 7740-5 (2010)

64. Kitagawa, T. & T. Ogura: Oxygen activation mechanism at the binuclear site of heme-copper oxidase superfamily as revealed by time-resolved resonance Raman spectroscopy. In: Progress in Inorganic Chemistry. Ed: K. D. Karlin. Wiley&Sons, Inc., (1997)

65. Ogura, T., S. Takahashi, K. Shinzawa-Itoh, S. Yoshikawa & T. Kitagawa: Observation of the Fe^{4+}=0 stretching Raman band for cytochrome oxidase compound B at ambient temperature. *J Biol Chem*, 265, 14721-14723 (1990)

66. Wiertz, F. G. M., O.M. H. Richter, A. V. Cherepanov, F. MacMillan, B. Ludwig & S. de Vries: An oxo-ferryl tryptophan radical catalytic intermediate in cytochrome *c* and quinol oxidases trapped by microsecond freeze-hyperquenching (MNQ) *FEBS Lett*, 575, 127-130 (2004)

67. Siegbahn, P. & M. R. A. Blomberg: Important roles of tyrosines in Photosystem II and cytochrome oxidase. *Biochim Biophys Acta*, 1655, 45-50 (2004)

68. MacMillan, F., K. Budiman, H. Angerer & H. Michel: The role of triptophan 272 in the *Paracoccus denitrificans* cytochrome *c* oxidase. *FEBS Lett*, 580, 1345-1349 (2006)

69. Wiertz, F. G. M., O.-M. H. Richter, B. Ludwig & S. de Vries: Kinetic resolution of a tryptophan-radical intermediate in the reaction cycle of *Paracoccus denitrificans* cytochrome *c* oxidase *J Biol Chem*, 282, 31580-31591 (2007)

70. Gorbikova, E. A., I. Belevich, M. Wikstrom & M. I. Verkhovsky: The proton donor for O-O bond scission by cytochrome *c* oxidase. *Proc Natl Acad Sci USA*, 105, 10733-10737 (2008)

71. Oliveberg, M., P. Brzezinski & B. G. Malmstrom: The effect of pH and temperature on the reaction of fully reduced and mixed-valence cytochrome *c* oxidase with dioxygen. *Biochem Biophys Acta*, 977, 322-328 (1989)

72. Verkhovsky, M. I., J. E. Morgan & M. Wikstrom: Oxygen binding and activation: early steps in the reaction of oxygen with cytochrome *c* oxidase. *Biochemistry*, 33, 3079-3086 (1994)

73. Siletsky, S. A., D. Han, S. Brand , J. E. Morgan, M. Fabian, L. Geren , F. Millett , B. Durham , A. A. Konstantinov & R. B. Gennis: Single-electron photoreduction of the P_M intermediate of cytochrome *c* oxidase. *Biochim Biophys Acta*, 1757, 1122–1132 (2006)

74. Bloch, D., I. Belevich, A. Jasaitis, C. Ribacka, A. Puustinen, M. I. Verkhovsky & M. Wikstrom: The catalytic cycle of cytochrome *c* oxidase is not the sum of its two halves. *Proc Natl Acad Sci USA*, 101, 529-533 (2004)

75. Belevich, I., D. A. Bloch, M. Wikstrom & M. I. Verkhovsky: Exploring the proton pump mechanism of cytochrome *c* oxidase in real time. *Proc Natl Acad Sci U S A*, 104, 2685-2690 (2007)

76. Brand, S. E., S. Rajagukguk, K. Ganesan, L. Geren, M. Fabian, D. Han, R. B. Gennis, B. Durham & F. Millett: A new ruthenium complex to study single-electron reduction of the pulsed O_H state of detergent-solubilized cytochrome oxidase. *Biochemistry*, 46, 14610-14618 (2007)

77. Siletsky, S. A., I. Belevich, M. Wikstrom, T. Soulimane & M. I. Verkhovsky: Time-resolved O_H->E_H transition of the aberrant ba_3 oxidase from *Thermus thermophilus*. *Biochim Biophys Acta*, 1787, 201-5 (2009)

78. Siletsky, S. A., I. Belevich, N. P. Belevich, T. Soulimane & M. I. Verkhovsky: Time-resolved single-turnover of caa_3 oxidase from *Thermus thermophilus*. Fifth electron of the fully reduced enzyme converts O_H into E_H state. *Biochim Biophys Acta*, 1807, 1162-1169 (2011)

79. Siletsky, S., A. D. Kaulen & A. A. Konstantinov: Resolution of electrogenic steps coupled to conversion of cytochrome *c* oxidase from the peroxy to the ferryl-oxo state. *Biochemistry*, 38, 4853-4861 (1999)

80. Verkhovsky, M. I., A. Tuukkanen, C. Backgren, A. Puustinen & M. Wikstrom: Charge translocation coupled to electron injection into oxidized cytochrome *c* oxidase from *Paracoccus denitrificans*. *Biochemistry*, 40, 7077-7083 (2001)

81. Jancura, D., V. Berka, M. Antalik, J. Bagelova, R. B. Gennis, G. Palmer & M. Fabian: Spectral and kinetic equivalence of oxidized cytochrome *c* oxidase as isolated and "activated" by reoxidation. *J Biol Chem*, 281, 30319–30325 (2006)

82. Gibson, Q. H. & C. Greenwood: Reactions of cytochrome oxidase with oxygen and carbon monoxide. *Biochem J*, 86, 541-554 (1963)

83. Blackmore, R. S., C. Greenwood & Q. H. Gibson: Studies of the primary oxygen intermediate in the reaction of fully reduced cytochrome oxidase. *J Biol Chem*, 266, 19245-19249 (1991)

84. Winkler, J. R., D. G. Nocera, K. M. Yocom, E. Bordignon & H. B. Gray: Electron-transfer kinetics of pentaammineruthenium(III)(histidine-33)-ferricytochrome *c*. Measurement of the rate of intramolecular electron transfer between redox centers separated by 15 A in a protein. *J Am Chem Soc*, 104, 5798-5800 (1982)

85. Pan, L. P., M. Frame, B. Durham, D. Davis & F. Millett: Photoinduced electron transfer within complexes between plastocyanin and ruthenium bisbipyridine dicarboxybipyridine cytochrome *c* derivatives. *Biochemistry*, 29, 3231-3236 (1990)

86. Pan, L. P., S. Hibdon, R.-Q. Liu, B. Durham & F. Millett: Intracomplex Electron Transfer Between Ruthenium-Cytochrome *c* Derivatives and Cytochrome *c* Oxidase. *Biochemistry*, 32, 8492-8498 (1993)

87. Nilsson, T.: Photoinduced electron transfer from tris(2,2'-bipyridyl)ruthenium to cytochrome *c* oxidase. *Proc Natl Acad Sci USA*, 89, 6497-6501 (1992)

88. Millett, F. & B. Durham: Photoinduced electron transfer reactions in metalloprotein complexes labeled with ruthenium polypyridine. In: Metal Ions in Biological Systems. Eds: H. Sigel&A. Siegel. Marcel Dekker, Inc., Basel, Switzerland (1991)

89. Geren, L., B. Durham & F. Millett: Use of ruthenium photoreduction techniques to study electron transfer in cytochrome oxidase. *Methods Enzymol*, 456, 507-520 (2009)

90. Kobayashi, K., H. Une & K. Hayashi: Electron transfer process in cytochrome oxidase after pulse radiolysis. *J Biol Chem*, 246, 7976-7980 (1989)

91. Farver, O., Y. Chen, J. A. Fee & I. Pecht: Electron transfer among the CuA-, heme *b*- and *a3*-centers of *Thermus thermophilus* cytochrome *ba*3. *FEBS Lett*, 580, 3417–3421 (2006)

92. Drachev, L. A., A. A. Jasaitis, A. D. Kaulen, A. A. Kondrashin, E. A. Liberman, I. B. Nemecek, S. A. Ostroumov, A. Semenov & V. P. Skulachev: Direct measurement of electric current generation by cytochrome oxidase, H+-ATPase and bacteriorhodopsin. *Nature*, 249, 321-4 (1974)

93. Drachev, L. A., A. D. Kaulen, A. Y. Semenov, I. I. Severina & V. P. Skulachev: Lipid-impregnated filters as a tool for studying the electric current-generating proteins. *Anal Biochem*, 96, 250-262 (1979)

94. Zaslavsky, D., A. Kaulen, I. A. Smirnova, T. V. Vygodina & A. A. Konstantinov: Flash-induced membrane potential generation by cytochrome *c* oxidase. *FEBS Lett*, 336, 389-393 (1993)

95. Verkhovsky, M. I., J. E. Morgan, M. Verkhovskaya & M. Wikstrom: Translocation of electrical charge during a single turnover of cytochrome *c* oxidase. *Biochim Biophys Acta*, 1318, 6-10 (1997)

96. Zaslavsky, D. L., I. A. Smirnova, S. A. Siletsky, A. D. Kaulen, F. Millett & A. A. Konstantinov: Rapid kinetics of membrane potential generation by cytochrome *c* oxidase with the photoactive Ru(II)-tris-bipyridyl derivative of cytochrome *c* as electron donor. *FEBS Lett*, 359, 27-30 (1995)

97. Siletsky, S. A., A. D. Kaulen & A. A. Konstantinov: Electrogenic events associated with peroxy- to ferryl-oxo state transition in cytochrome *c* oxidase. *Eur J Biophys*, 26, 98 (1997)

98. Siletsky, S. A., A. D. Kaulen, D. Mitchell, R. B. Gennis & A. A. Konstantinov: Resolution of two proton conduction pathways in cytochrome c oxidase. *EBEC Short Reports*, 9, 90 (1996)

99. Siletsky, S. A., A. S. Pawate, K. Weiss, R. B. Gennis & A. A. Konstantinov: Transmembrane charge separation during the ferryl-oxo-> oxidized transition in a non-pumping mutant of cytochrome *c* oxidase. *J Biol Chem*, 279, 52558-52565 (2004)

100. Siletsky, S. A., J. Zhu, R. B. Gennis & A. A. Konstantinov: Partial steps of charge translocation in the nonpumping N139L mutant of *Rhodobacter sphaeroides* cytochrome *c* oxidase with a blocked D-channel. *Biochemistry*, 49, 3060-73 (2010)

101. Ruitenberg, M., A. Kannt, E. Bamberg, B. Ludwig, H. Michel & K. Fendler: Single-electron reduction of the oxidized state is coupled to proton uptake via the K pathway in *Paracoccus denitrificans* cytochrome *c* oxidase. *Proc Natl Acad Sci USA*, 97, 4632-4636 (2000)

102. Ruitenberg, M., A. Kannt, E. Bamberg, K. Fendler & H. Michel: Reduction of cytochrome c oxidase by a second electron leads to proton translocation. *Nature*, 417, 99-102 (2002)

103. Jasaitis, A., M. I. Verkhovsky, J. E. Morgan, M. L. Verkhovskaya & M. Wikstrom: Assignment and charge translocation stoichiometries of the electrogenic phases in the reaction of cytochrome *c* with dioxygen. *Biochemistry*, 38, 2697-2706 (1999)

104. Ribacka, C., M. I. Verkhovsky, I. Belevich, D. A. Bloch, A. Puustinen & M. Wikstrom: An elementary reaction step of the proton pump is revealed by mutation of tryptophan-164 to phenylalanine in cytochrome *c* oxidase from *Paracoccus denitrificans*. *Biochemistry*, 44, 16502-16512 (2005)

105. Lepp, H. & P. Brzezinski: Internal charge transfer in cytochrome c oxidase at a limited proton supply: Proton pumping ceases at high pH. *Biochim Biophys Acta*, 1790, 552-557 (2009)

106. Chance, B., C. Saronio & J. S. Leigh, Jr.: Functional intermediates in the reaction of membrane-bound cytochrome oxidase with oxygen. *J Biol Chem*, 250, 9226-9237 (1975)

107. Han, S., Y.-C. Ching & D. L. Rousseau: Primary intermediate in the reaction of oxygen with fully reduced cytochrome *c* oxidase. *Proc Natl Acad Sci USA*, 87, 2491-2495 (1990)

108. Varotsis, C., W. H. Woodruff & G. T. Babcock: Direct detection of a dioxygen adduct of cytochrome a_3 in the mixed valence cytochome oxidase/dioxygen reaction. *J Biol Chem*, 265, 11131-11136 (1990)

109. Woodruff, W. H.: Coordination dynamics of heme-copper oxidases. The ligand shuttle and the control and coupling of electron transfer and proton translocation. *J Bioenerg Biomembr*, 25, 177-188 (1993)

110. Belevich, I., A. Tuukkanen, M. Wikstrom & M. I. Verkhovsky: Proton-coupled electron equilibrium in soluble and membrane-bound cytochrome *c* oxidase from *Paracoccus denitrificans*. *BIochemistry*, 45, 4000-4006 (2006)

111. Belevich, I., M. I. Verkhovsky & M. Wikstrom: Proton-coupled electron transfer drives the proton pump of cytochrome *c* oxidase. *Nature*, 440|, 829-832 (2006)

112. Popovic, D. M. & A. A. Stuchebrukhov: Electrostatic study of the proton pumping mechanism in bovine heart cytochrome *c* oxidase. *J Am Chem Soc*, 126, 1858-71 (2004)

113. Lepp, H., E. Svahn, K. Faxen & P. Brzezinski: Charge transfer in the K proton pathway linked to electron transfer to the catalytic site in cytochrome *c* oxidase. *Biochemistry*, 47, 4929-4935 (2008)

114. Gorbikova, E. A., M. Wikstrom & M. I. Verkhovsky: The protonation state of the cross-linked tyrosine during the catalytic cycle of cytochrome *c* oxidase. *J Biol Chem.*, 283, 34907-34912 (2008)

115. Siletsky, S. A., I. Belevich, A. Jasaitis, A. A. Konstantinov, M. Wikstrom, T. Soulimane & M. I. Verkhovsky: Time-resolved single-turnover of ba_3 oxidase from *Thermus thermophilus*. *Biochim Biophys Acta*, 1767, 1383-92 (2007)

116. Jasaitis, A., C. Backgren, J. E. Morgan, A. Puustinen, M. I. Verkhovsky & M. Wikstrom: Electron and proton transfer in the arginine-54-methionine mutant of cytochrome *c* oxidase from *Paracoccus denitrificans*. *Biochemistry*, 40, 5269-5274 (2001)

117. Belevich, I., E. Gorbikova, N. P. Belevich, V. Rauhamaki, M. Wikstrom & M. I. Verkhovsky: Initiation of the proton pump of cytochrome c oxidase. *Proc Natl Acad Sci U S A*, 107, 18469-74 (2010)

118. Hinkle, P. & P. Mitchell: Effect of membrane potential on the redox poise between cytochrome *a* and cytochrome *c* in rat liver mitochondria. *J Bioenerg* 1, 45-60 (1970)

119. Tsukihara, T., H. Aoyama, E. Yamashita, T. Tomizaki, H. Yamaguchi, K. Shinzawa-Itoh, T. Nakashima, R. Yaono & S. Yoshikawa: Structures of metal sites of oxidized bovine heart cytochrome *c* oxidase at 2.8 A. *Science*, 269, 1069-1074 (1995)

120. Verkhovsky, M. I., A. Jasaitis, M. L. Verkhovskaya, L. Morgan & M. Wikstrom: Proton translocation by cytochrome *c* oxidase. *Nature*, 400, 480-483 (1999)

121. Faxen, K., G. Gilderson, P. Adelroth & P. Brzezinski: A mechanistic principle for proton pumping by cytochrome *c* oxidase. *Nature*, 437, 286-289 (2005)

122. Siletsky, S. A., D. Han, S. Brand, J. E. Morgan, M. Fabian, L. Geren, F. Millett, B. Durham, A. A. Konstantinov & R. B. Gennis: Single-electron photoreduction of the P_M intermediate of cytochrome *c* oxidase. *Biochim Biophys Acta*, 1757, 1122-32 (2006)

123. Kaila, V. R., M. I. Verkhovsky & M. Wikstrom: Proton-coupled electron transfer in cytochrome oxidase. *Chem Rev*, 110, 7062-81 (2010)

124. Smirnova, I., P. Adelroth, R. B. Gennis & P. Brzezinski: Aspartate-132 in cytochrome *c* oxidase from *Rhodobacter sphaeroides* is involved in a two-step proton transfer during oxo-ferryl formation. *Biochemistry*, 38, 6826-6833 (1999)

125. Namslauer, A., A. Pawate, R. Gennis & P. Brzezinski: Redox-coupled proton translocation in biological systems: Proton shuttling in cytochrome *c* oxidase. *Proc Natl Acad Sci USA*, 100, 15543-15547 (2003)

126. Gorbikova, E. A., N. P. Belevich, M. Wikstrom & M. I. Verkhovsky: Time-resolved ATR-FTIR spectroscopy of the oxygen reaction in the D124N mutant of cytochrome *c* oxidase from *Paracoccus denitrificans*. *Biochemistry*, 46, 13141-13148 (2007)

127. Branden, G., R. B. Gennis & P. Brzezinski: Transmembrane proton translocation by cytochrome *c* oxidase. *Biochim Biophys Acta*, 1757, 1052–1063 (2006)

128. Zaslavsky, D., R. C. Sadoski, K. Wang, B. Durham, R. B. Gennis & F. Millett: Single electron reduction of cytochrome *c* oxidase compound F: resolution of partial steps by transient spectroscopy. *Biochemistry*, 37, 14910-14916 (1998)

129. Weng, L. & G. M. Baker: Reaction of hydrogen peroxide with the rapid form of resting cytochrome oxidase. *Biochemistry*, 30, 5727-5733 (1991)

130. Siletsky, S., D. Zaslavsky, I. Smirnova, A. Kaulen & A. Konstantinov: F-to-O transition of cytochrome *c* oxidase: pH and temperature effects on kinetics of charge translocation *Biochem Soc Trans*, 28, A457 (2000)

131. Farver, O., S. Wherland, W. E. Antholine, G. J. Gemmen, Y. Chen, I. Pecht & J. A. Fee: Pulse radiolysis studies of temperature dependent electron transfers among redox centers in ba_3-cytochrome *c* oxidase from *Thermus thermophilus*: comparison of A- and B-type enzymes. *Biochemistry*, in press, (2010)

132. Laidler, K. J.: Unconvenitonal applications of the Arrhenius Law *J Chem Educ* 49, 343-344 (1972)

133. Moser, C. C., C. C. Page & P. L. Dutton: Darwin at the molecular scale: selection and variance in electron tunnelling proteins including cytochrome c oxidase. *Philos Trans R Soc Lond B Biol Sci*, 361, 1295-1305 (2006)

134. Tittor, J., C. Soell, D. Oesterhelt, H. J. Butt & E. Bamberg: A defective proton pump, point-mutated bacteriorhodopsin Asp96-Asn is fully reactivated by azide. *EMBO J*, 8, 3477-3482 (1989)

135. Gopta, O. A., D. A. Bloch, D. A. Cherepanov & A. Y. Mulkidjanian: Temperature dependence of the electrogenic reaction in the Q_B site of the *Rhodobacter sphaeroides* photosynthetic reaction center: the Q_A-Q_B -> Q_AQ_B- transition. *FEBS Lett*, 412, 490-494 (1997)

136. Decoursey, T. E.: Voltage-gated proton channels and other proton transfer pathways. *Physiol Rev*, 83, 475-579 (2003)

137. Mamedov, M. D., A. A. Tyunyatkina, S. A. Siletsky & A. Y. Semenov: Voltage changes involving photosystem II quinone-iron complex turnover. *Eur Biophys J*, 35, 647-654 (2006)

138. Kozlova, M. A., H. D. Juhnke, D. A. Cherepanov, C. R. Lancaster & A. Y. Mulkidjanian: Proton transfer in the photosynthetic reaction center of *Blastochloris viridis*. *FEBS Lett*, 582, 238-242 (2008)

139. Maroti, P. & C. A. Wraight: Kinetics of H^+ ion binding by the $P^+Q_A^-$state of bacterial photosynthetic reaction centers: rate limitation within the protein. *Biophys J*, 73, 367-381 (1997)

140. Kuznetsova, S. S., N. V. Azarkina, T. V. Vygodina, S. A. Siletsky & A. A. Konstantinov: Zinc ions as cytochrome *c* oxidase inhibitors: two sites of action. *Biochemistry (Mosc)*, 70, 128-136 (2005)

141. Paddock, M. L., M. S. Graige, G. Feher & M. Y. Okamura: Identification of the proton pathway in bacterial reaction centers: inhibition of proton transfer by binding of Zn^{2+} or Cd^{2+}. *Proc Natl Acad Sci U S A*, 96, 6183-6188 (1999)

142. Link, T. A. & G. von Jagow: Zinc ions inhibit the Q_P center of bovine heart mitochondrial bc_1 complex by blocking a protonatable group. *J Biol Chem*, 270, 25001-25006 (1995)

143. Kannt, A., T. Ostermann, H. Muller & M. Ruitenberg: Zn^{2+} binding to the cytoplasmic side of *Paracoccus denitrificans* cytochrome *c* oxidase selectively uncouples electron transfer and proton translocation. *FEBS Lett*, 503, 142-146 (2001)

144. Aagaard, A., A. Namslauer & P. Brzezinski: Inhibition of proton transfer in cytochrome *c* oxidase by zinc ions: delayed proton uptake during oxygen reduction. *Biochim Biophys Acta*, 1555, 133-139 (2002)

145. Siletsky, S. A., A. D. Kaulen & A. A. Konstantinov: Electrogenic events associated with peroxy-to-ferryl-oxo state transition in cytochrome c oxidase. *Eur J Biophys*, 26, 98 (1997)

146. Verkhovsky, M. I., I. Belevich, D. A. Bloch & M. Wikstrom: Elementary steps of proton translocation in the catalytic cycle of cytochrome oxidase. *Biochim Biophys Acta*, 1757, 401–407 (2006)

147. Medvedev, D. M., E. S. Medvedev, A. I. Kotelnikov & A. A. Stuchebrukhov: Analysis of the kinetics of the membrane potential generated by cytochrome *c* oxidase upon single electron injection. *Biochim Biophys Acta*, 1710, 47-56 (2005)

148. Hill, B. C. & C. Greenwood: The reaction of fully reduced cytochrome *c* oxidase with oxygen studied by flow-flash spectrophotometry at room temperature. *Biochem J*, 218, 913-921 (1984)

149. Sharpe, M. A. & S. Ferguson-Miller: A chemically explicit model for the mechanism of proton pumping in heme-copper oxidases. *J Bioenerg Biomembr*, 40, 541-549 (2008)

150. Adelroth, P., R. B. Gennis & P. Brzezinski: Role of the pathway through K(I-362) in proton transfer in cytochrome *c* oxidase from *R. sphaeroides*. *Biochemistry*, 37, 2470-2476 (1998)

151. Wikstrom, M. K. F., A. Jasaitis, C. Backgren, A. Puustinen & M. I. Verkhovsky: The role of the D- and K-pathways of proton transfer in the function of the haem-copper oxidases. *Biochim Biophys Acta*, 1459, 514-520 (2000)

152. Pfitzner, U., K. Hoffmeier, A. Harrenga, A. Kannt, H. Michel, E. Bamberg, O.-M. H. Richter & B. Ludwig: Tracing the D-pathway in reconstituted site-directed mutants of cytochrome *c* oxidase from *Paracoccus denitrificans*. *Biochemistry*, 39, 6756-6762 (2000)

153. Pawate, A. S., J. Morgan, A. Namslauer, D. Mills, P. Brzezinski, S. Ferguson-Miller & R. B. Gennis: A mutation in subunit I of cytochrome oxidase from *Rhodobacter sphaeroides* results in an increase in steady-state activity but completely eliminates proton pumping. *Biochemistry*, 41, 13417-13423. (2002)

154. Salomonsson, L., K. Faxen, P. Adelroth & P. Brzezinski: The timing of proton migration in membrane-reconstituted cytochrome *c* oxidase. *Proc Natl Acad Sci U S A*, 102, 17624-17629 (2005)

155. Siletsky, S., F. Thomson, R. Gennis, A. D. Kaulen & A. Konstantinov: Time-resolved studies of intraprotein proton transfer in the D-channel mutants of *Rhodobacter sphaeroides* cytochrome *c* oxidase. *Biochim Biophys Acta, EBEC Short Reports*, 1555, 114 (2002)

156. Adelroth, P., M. Svensson-Ek, D. M. Mitchell, R. B. Gennis & P. Brzezinski: Glutamate 286 in cytochrome aa_3 from *Rhodobacter sphaeroides* is involved in proton uptake during the reaction of the fully-reduced enzyme with dioxygen. *Biochemistry*, 36, 13824-13829 (1997)

157. Siletsky, S. & A. A. Konstantinov: Electrogenic mechanism of cytochrome *c* oxidase. *The 8th European Biological Chemistry Conference,* 80 (2006)

158. Sadoski, R. C., D. Zaslavsky, R. B. Gennis, B. Durham & F. Millett: Exposure of bovine cytochrome *c* oxidase to high triton X-100 or to alkaline conditions causes a dramatic change in the rate of reduction of compound F. *J Biol Chem*, 276, 33616-33620 (2001)

159. Wikstrom, M., K. Krab & M. Saraste: Cytochrome oxidase - a synthesis. Academic Press, New York (1981)

160. Brzezinski, P. & G. Larsson: Redox-driven proton pumping by heme-copper oxidases. *Biochim Biophys Acta*, 1605, 1-13 (2003)

161. Kaila, V. R., M. I. Verkhovsky, G. Hummer & M. Wikstrom: Glutamic acid 242 is a valve in the proton pump of cytochrome *c* oxidase. *Proc Natl Acad Sci U S A*, 105, 6255-6259 (2008)

162. Olsson, M. H. M., P. K. Sharma & A. Warshel: Simulating redox coupled proton transfer in cytochrome *c* oxidase: looking for the proton bottleneck. *FEBS Lett.*, 579, 2026-2034 (2005)

163. Yoshikawa, S.: A cytochrome *c* oxidase proton pumping mechanism that excludes the O2 reduction site. *FEBS Lett.*, 555, 8-12 (2003)

164. Papa, S., N. Capitanio & G. Capitanio: A cooperative model for proton pumping in cytochrome *c* oxidase. *Biochim Biophys Acta*, 1655, 353-364 (2004)

165. Namslauer, A. & P. Brzezinski: Structural elements involved in electron-coupled proton transfer in cytochrome *c* oxidase. *FEBS Lett*, 567, 103-110 (2004)

166. Seibold, S. A., D. A. Mills, S. Ferguson-Miller & R. I. Cukier: Water chain formation and possible proton pumping routes in *Rhodobacter sphaeroides* cytochrome *c* oxidase: a molecular dynamics comparison of the wild type and R481K mutant. *Biochemistry*, 44, 10475-10485 (2005)

167. Wikstrom, M.: Mechanism of proton translocation by cytochrome *c* oxidase: a new four-stroke histidine cycle. *Biochim Biophys Acta*, 1458, 188-198 (2000)

168. Kannt, A., T. Soulimane, G. Buse, A. Becker, E. Bamberg & H. Michel: Electrical current generation and proton pumping catalyzed by the ba_3-type cytochrome *c* oxidase from *Thermus thermophilus*. *FEBS Lett*, 434, 17-22 (1998)

169. Siletskiy, S., T. Soulimane, N. Azarkina, T. V. Vygodina, G. Buse, A. Kaulen & A. Konstantinov: Time-resolved generation of membrane potential by ba_3 cytochrome c oxidase from *Thermus thermophilus*. Evidence for reduction-induced opening of the binuclear centre. *FEBS Lett*, 457, 98-102 (1999)

170. von Ballmoos, C., R. B. Gennis, P. Adelroth & P. Brzezinski: Kinetic design of the respiratory oxidases. *Proc Natl Acad Sci U S A*, 108, 11057-11062 (2011)

171. Chakrabarty, S., I. Namslauer, P. Brzezinski & A. Warshel: Exploration of the cytochrome *c* oxidase pathway puzzle and examination of the origin of elusive mutational effects. *Biochim Biophys Acta*, 1807, 413-426 (2011)

172. Henry, R. M., C.-H. Yu, T. Rodinger & R. Pomes: Functional Hydration and Conformational Gating of Proton Uptake in Cytochrome c Oxidase. *J. Mol. Biol.*, 387, 1165-1185 (2009)

173. Humphrey, W., A. Dalke & K. Schulten: VMID visual molecular dynamics. *J. Mol. Graph.*, 14, 33- (1996)

174. Siletsky, S. A.: Studies of electrogenic transfer of protons in cytochrome oxidase. Moscow State University, 108 (1998)

Abbreviations: COX: cytochrome oxidase, PLS: proton loading site, BNC: binuclear catalytic centre, Rubpy: tris(2,2-bipyridyl)ruthenium, r.a.: relative amplitude

Key Words: Cytochrome, Oxidase, Protons, Membrane potential, Channels, Electrogenic, Voltage, Electron injection, Review

Send correspondence to: Sergey A. Siletsky, A.N.Belozersky Institute of Physico-Chemical Biology, Moscow State University, Moscow 119992, Russia, Tel: 7 495 939 51 49, Fax: 7 495 939 31 81, E-mail: siletsky@genebee.msu.su